Error Estimates for Adaptive Spectral Decompositions

Daniel H. Baffet, Yannik G. Gleichmann, Marcus J. Grote

Departement Mathematik und Informatik
Fachbereich Mathematik
Universität Basel
CH-4051 Basel

Preprint No. 2022-01
January 2022

dmi.unibas.ch

Error estimates for Adaptive Spectral Decompositions

Daniel H. Baffet [*†] Yannik G. Gleichmann [*‡] Marcus J. Grote [*§]

July 30, 2021

Abstract

Adaptive spectral (AS) decompositions associated with a piecewise constant function, u, yield small subspaces where the characteristic functions comprising u are well approximated. When combined with Newton-like optimization methods, AS decompositions have proved remarkably efficient in providing at each nonlinear iteration a low-dimensional search space for the solution of inverse medium problems. Here, we derive L^2-error estimates for the AS decomposition of u, truncated after K terms, when u is piecewise constant and consists of K characteristic functions over Lipschitz domains and a background. Numerical examples illustrate the accuracy of the AS decomposition for media that either do, or do not, satisfy the assumptions of the theory.

Keywords: Inverse medium problem, scattering problem, adaptive eigenspace inversion, image segmentation

1 Introduction

Adaptive spectral (AS) decompositions have been proposed as low-dimensional search spaces during the iterative solution of inverse medium problems [1–5]. For piecewise constant media, in particular, AS decompositions have proved remarkably efficient and accurate. So far, however, their remarkable approximation properties are only supported by numerical evidence. Here, starting from [5], we derive L^2 error estimates for AS approximations of piecewise constant functions.

In [1], De Buhan and Osses proposed to restrict the search space of an inverse medium problem to the span of a small basis of eigenfunctions of a judicious elliptic operator, repeatedly adapted during the nonlinear iteration. Their adaptive inversion approach relies on a decomposition

$$v = \sum_{k=1}^{\infty} \beta_k \varphi_k, \tag{1.1}$$

for $v \in W_0^{1,\infty}(\Omega)$, with $\Omega \subset \mathbb{R}^d$. Here each φ_k is an eigenfunction of a v-dependent, linear, symmetric, and elliptic operator $L_\varepsilon[v]$, i.e.,

$$L_\varepsilon[v]\varphi_k = \lambda_k \varphi_k \quad \text{in } \Omega, \qquad \varphi_k = 0 \quad \text{on } \partial\Omega, \tag{1.2}$$

[*]Department of Mathematics and Computer Science, University of Basel, Basel, Switzerland
[†]daniel.baffet@unibas.ch
[‡]yannik.gleichmann@unibas.ch
[§]marcus.grote@unibas.ch

for an eigenvalue $\lambda_k \in \mathbb{R}$. In the sequel we shall in fact apply the AS decomposition to more general functions in $W^{1,\infty}(\Omega)$ by extending their boundary data appropriately into the interior of Ω; here, for simplicity, we suppose $v \in W_0^{1,\infty}(\Omega)$.

Clearly, the choice of $L_\varepsilon[v]$ is crucial for obtaining an efficient approximation of v with as few basis functions as possible. Typically, we use

$$L_\varepsilon[v]w = -\nabla\cdot\left(\mu_\varepsilon[v]\nabla w\right), \qquad \mu_\varepsilon[v](x) = \frac{1}{\sqrt{|\nabla v(x)|^2 + \varepsilon^2}}, \tag{1.3}$$

where $\varepsilon > 0$ is a small parameter to avoid division by zero, but other forms have also been used in the past and are treated by our analysis.

Note that we cannot apply the above AS decomposition directly to piecewise constant u, because $\mu_\varepsilon[u]$ is not in L^∞ and thus $L_\varepsilon[u]$ not well-defined. Nevertheless, we may still (approximately) decompose u at the cost of an additional step. We first approximate u by a more regular approximation, which we denote generically by u_δ, where $\delta > 0$ is a parameter that controls the error and is proportional to the width of the support of ∇u_δ near the jump discontinuities of u. Then we apply the AS decomposition to u_δ and obtain an approximation of u by truncating the expansion (1.1) in the eigenfunctions of $L_\varepsilon[u_\delta]$.

Insight about the AS decomposition approach may be obtained from its connection to the total variation (TV) functional, which is commonly used for image denoising while preserving edges. In fact, $L_\varepsilon[v]v$, with $L_\varepsilon[v]$ given by (1.3), is the FrÃľchet derivative of the penalized TV functional – see [3, Remark 1]. The eigenvalue problem for $L_\varepsilon[v]$ also bears a striking resemblance to nonlinear eigenvalue problems for the TV functional, which have been studied in the more general context of 1-homogeneous functionals for image processing – see [6–8] and the references therein. In particular, the characteristic functions of convex bounded domains in the plane with a sufficiently regular boundary are eigenfunctions of the TV functional [8] – see also [5, Remark 8].

The AS decomposition has been used as follows in various iterative Newton-like algorithms for the solution of inverse medium problems [2–4]: Given an approximation of the medium, $u^{(m-1)}$, from the previous iteration, the approximation $u^{(m)}$ at the current iteration is set as the minimizer of the misfit in the space $\text{span}(\varphi_k)_{k=1}^K$, where φ_k, $k = 1, \dots, K$, satisfy (1.2) with $v = u^{(m-1)}$. As the approximation $u^{(m)}$ changes from one iteration to the next, so does the search space used for the subsequent minimization.

By combining the adaptive inversion process with the TRAC (time reversed absorbing condition) approach, de Buhan and Kray [2] developed an effective solution strategy for time-dependent inverse scattering problems. In [3], Grote, Kray and Nahum proposed the AEI (adaptive eigenspace inversion) algorithm for inverse scattering problems in the frequency domain. In [4], the AEI algorithm was extended to multi-parameter inverse medium problems. Recently, it was extended to electromagnetic inverse scattering problems at fixed frequency [9] and also to time-dependent inverse scattering problems when the illuminating source is unknown [10]. In [11], AS decompositions were used for solving 2-D and 3-D seismic inverse problems for the Helmholtz equation. First theoretical estimates for AS decompositions together with an approach for adapting the dimension of the search space were derived in [5].

When u consists of a sum of K characteristic functions of sets compactly contained in Ω, the expansion (1.1) in the spectral basis of $L_\varepsilon[u_\delta]$ truncated after K terms has proved remarkably accurate, as it essentially recovers u. In [5] it is shown that the gradients of the first K eigenfunctions of $L_\varepsilon[u_\delta]$ are small away from the discontinuities of u. Thus, in regions where u is constant, each φ_k ($k = 1, \ldots, K$) is also nearly constant and we expect that u be well approximated in $\Phi_K^{\varepsilon,\delta} = \text{span}\{\varphi_k\}_{k=1}^K$. Here, our goal is to rigorously prove this proposition.

The remainder of our paper is organized as follows. In Section 2, we describe the class of piecewise constant media considered, provide definitions and introduce notation. In fact, we consider the more general case when u is not necessarily constant near the boundary $\partial\Omega$. Section 3 contains the analysis and the main results of the paper. Starting from the estimates of the gradients of $\varphi_1, \ldots, \varphi_K$ obtained in [5], we derive L^2 estimates for the projection error of u onto the appropriate affine space. In our main result, given by Theorem 3.6, we then prove that the L^2 projection error of u is $\mathcal{O}(\sqrt{\varepsilon + \delta})$. Moreover, we show that any of the K characteristic functions composing u is approximated by its L^2 projection on $\Phi_K^{\varepsilon,\delta}$ up to $\mathcal{O}(\sqrt{\varepsilon + \delta})$. That proof also requires a technical result about the level sets of distance functions for Lipschitz domains, which is provided in Appendix B. Finally, we present in Section 4 various numerical examples which illustrate the accuracy of the AS decomposition for media that either do, or do not, satisfy the assumptions of our theory.

2 Notation and definitions

The AS decomposition (1.1) of a function v is based on the spectral decomposition of the v-dependent operator $L_\varepsilon[v]$ given by

$$L_\varepsilon[v]w = -\nabla\cdot(\mu_\varepsilon[v]\nabla w)\,. \tag{2.1}$$

Typically, the weight function $\mu_\varepsilon[v]$ has the form of either

$$\mu_\varepsilon[v](x) = \frac{1}{(|\nabla v(x)|^q + \varepsilon^q)^{1/q}}\,, \tag{2.2}$$

for some $q \in [1, \infty)$, or

$$\mu_\varepsilon[v](x) = \frac{1}{\max\{|\nabla v(x)|,\, \varepsilon\}}\,. \tag{2.3}$$

For the analysis below, however, we allow more general $\mu_\varepsilon[v]$.

Suppose we wish to decompose a piecewise constant function u into the characteristic functions composing it. Note that we cannot apply the AS decomposition directly to u: since u is piecewise constant, $\mu_\varepsilon[u]$ is not in L^∞, and so $L_\varepsilon[u]$ is not well defined. Nevertheless, we may still (approximately) decompose u at the cost of an additional step. We first approximate u by a more regular approximation, which we denote generically by u_δ, where δ is a parameter that controls the error and is proportional to the width of the support of ∇u_δ near the jump discontinuities of u. Then we may apply the AS decomposition to u_δ and obtain an approximation of u by truncating the expansion.

To include finite element (FE) approximations in the analysis, we formulate boundary value problems in closed subspaces $\mathcal{V}^\delta \subset H^1(\Omega)$ and $\mathcal{V}_0^\delta = \mathcal{V}^\delta \cap H_0^1(\Omega)$, respectively. We let $\langle\cdot,\cdot\rangle$ and $\|\cdot\|_{L^2(\Omega)}$ denote the standard inner product and norm of $L^2(\Omega)$, and $|\cdot|$ denote the ℓ^2-norm. We use C, C_1, C_2, etc. to denote generic constants which may depend on u, but are independent of δ and ε; their values may also vary depending on the context. We sometimes use the term "medium" to refer to functions on the domain of interest $\Omega \subset \mathbb{R}^d$.

2.1 Piecewise constant medium

Let $\Omega \subset \mathbb{R}^d$, with $d \geq 2$, be a bounded Lipschitz domain, and $u : \Omega \to \mathbb{R}$ be piecewise constant such that

$$u(x) = u^0(x) + \widetilde{u}(x), \qquad x \in \Omega, \tag{2.4}$$

where

$$u^0 = \sum_{m=1}^{M} \omega_m \chi_{\Omega^m}\,, \quad \omega_m \in \mathbb{R}, \qquad \widetilde{u} = \sum_{k=1}^{K} \alpha_k \chi_{A^k}\,, \quad \alpha_k \in \mathbb{R} \setminus \{0\}, \tag{2.5}$$

with χ_A denoting the characteristic function of a set $A \subset \mathbb{R}^d$. We suppose $\Omega^1, \ldots, \Omega^M$ are disjoint Lipschitz domains covering Ω,

$$\overline{\Omega} = \bigcup_{m=1}^{M} \overline{\Omega^m}.$$

To ensure that for each m, $\partial\Omega^m \cap \partial\Omega$ is open in the topology of $\partial\Omega$, we assume

$$\Omega^m = \Omega \cap \widetilde{\Omega}^m, \qquad \partial\Omega \cap \widetilde{\Omega}^m \neq \emptyset,$$

for some bounded disjoint Lipschitz domain $\widetilde{\Omega}^m \subset \mathbb{R}^d$. Moreover, we suppose $A^1, \ldots, A^K$ are Lipschitz domains with mutually disjoint boundaries such that for each k, the boundary ∂A^k of A^k is connected, and $A^k \subset\subset \Omega^m$ for some $m = 1, \ldots, M$. Hence Ω is partitioned into finitely many subdomains Ω^m adjacent to its boundary $\partial\Omega$, while each Ω^m may contain one or several inclusions A^k isolated from $\partial\Omega$.

2.2 Admissible approximation

Suppose u is approximated by $u_\delta \in \mathcal{V}^\delta \subset H^1(\Omega)$ in the sense that

$$\lim_{\delta\to 0} \|u_\delta - u\|_{L^2(\Omega)} = 0. \tag{2.6}$$

We assume u_δ is obtained by a method satisfying the conditions in Appendix A below, introduced in [5]. We refer to such methods as *admissible*.

In Corollary 6 of [5] we provide two examples of standard methods which are admissible:

Example 2.1. For $\delta > 0$, let V_δ denote an H^1-conforming FE space associated with a simplex mesh $\mathcal{T}_\delta$ with mesh size δ. If the family of meshes $\{\mathcal{T}_\delta\}_\delta$ is regular and quasi-uniform (see, e.g., [12]), then the interpolation u_δ of u in V_δ is admissible. The proof of this proposition requires technical yet standard arguments and is therefore omitted.

Example 2.2. If u is extended to $\mathbb{R}^d$ by

$$u = \sum_{m=1}^{M} \omega_m \chi_{\widetilde{\Omega}^m} + \sum_{k=1}^{K} \alpha_k \chi_{A^k} \tag{2.7}$$

(compare with (2.4), (2.5)), and u_δ is the convolution

$$u_\delta(x) = \zeta_\delta * u = \int_{\mathbb{R}^d} \zeta_\delta(x-y) u(y)\, dy, \qquad \zeta_\delta(x) = \delta^{-d}\zeta(x/\delta) \tag{2.8}$$

with ζ the standard mollifier (e.g., [13]), then u_δ is admissible. For the proof see Corollary 6 of [5].

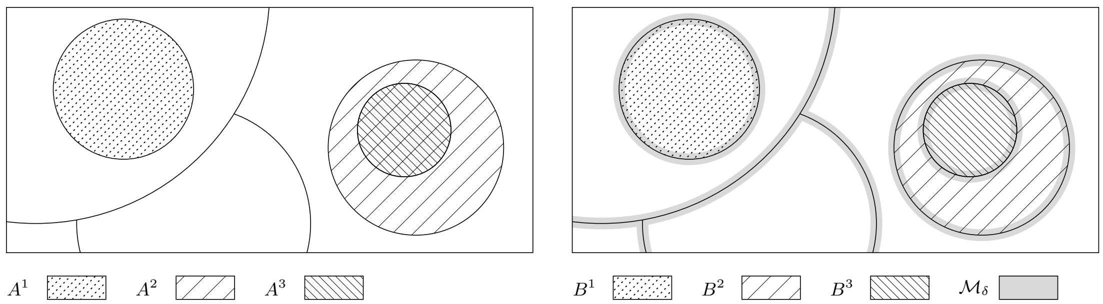

Figure 1: Typical configuration in two dimensions. In this example $K = 3$ and $M = 4$. The frame on the left shows the sets A^1, A^2 and A^3, and the frame on the right shows $B^1 = A^1$, $B^2 = A^2 \setminus A^3$, and $B^3 = A^3$.

We require u be obtained by an admissible method so we may employ the estimates obtained in [5]. However, for simplicity of presentation, here we state only conditions we directly use in this paper. We shall use that u_δ satisfies

$$\nabla u_\delta \in L^\infty(\Omega), \qquad \operatorname{supp}(\nabla u_\delta) \subset \mathcal{M}_\delta, \tag{2.9}$$

for the δ-wide neighborhood $\mathcal{M}_\delta$ of all interfaces, i.e.,

$$\mathcal{M}_\delta = \bigcup_{k=1}^{K} \{x \in \Omega : \ \operatorname{dist}(x, \partial A^k) < \delta\} \cup \bigcup_{m=1}^{M} \{x \in \Omega : \ \operatorname{dist}(x, \partial\Omega^m \cap \Omega) < \delta\}. \tag{2.10}$$

Here, $\operatorname{dist}(x, W)$ denotes the distance of $x \in \mathbb{R}^d$ to the set $W \subset \mathbb{R}^d$.

While $\nabla u_\delta \in L^\infty(\Omega)$, u_δ converges to a function u with jump discontinuities and therefore $\|\nabla u_\delta\|_{L^\infty(\Omega)}$ is generally not bounded with respect to δ. Still, we assume there exists a constant C, such that for every $\delta > 0$ sufficiently small, u_δ satisfies

$$\delta \|\nabla u_\delta\|_{L^\infty(\Omega)} \leq C. \tag{2.11}$$

For the analysis below it is convenient to partition the open complement,

$$D_\delta = \Omega \setminus \overline{\mathcal{M}_\delta}, \tag{2.12}$$

where $\nabla u_\delta = 0$ into its (disjoint) connected components. Hence, we let the sets $A^1, \dots, A^K$ be indexed so that if $i > k$, then either $A^i \subset A^k$ or $A^i \cap A^k = \emptyset$, and define

$$B^k_\delta = B^k \cap D_\delta, \qquad B^k = A^k \setminus \bigcup_{i>k} \overline{A^i}, \qquad k = 1, \dots, K. \tag{2.13}$$

Figure 1 shows an illustration of a possible configuration in 2 dimensions.

Similarly, we define outside the inclusions

$$E^m_\delta = E^m \cap D_\delta, \qquad E^m = \Omega^m \setminus \bigcup_{k=1}^{K} \overline{A^k}, \qquad m = 1, \dots, M. \tag{2.14}$$

Thus, for each k and $\delta > 0$ small, B^k and B^k_δ are open and connected, and D_δ is given by the disjoint union

$$D_\delta = E_\delta \cup \bigcup_{k=1}^{K} B^k_\delta,$$

where E_δ denotes the "δ-exterior",

$$E_\delta = \bigcup_{m=1}^{M} E^m_\delta. \tag{2.15}$$

By Theorem B.1, for every sufficiently small δ, each B^k_δ is a Λ-Lipschitz domain, for some Λ independent of δ. Note, however, that since a portion of the boundary of E^m_δ coincides with the boundary of E^m for every δ, it does not have the form assumed in Theorem B.1. As a result, we cannot rely on the same theorem to deduce that E^m_δ is a Lipschitz domain. Nevertheless, outside a neighborhood of $\partial\Omega \cap \partial E^m$, the boundary of E^m_δ is a Λ-Lipschitz surface with E^m_δ lying to one of its sides, by Theorem B.6. It is therefore possible to modify the definition of $\mathcal{M}_\delta$ so that for every δ sufficiently small, E^m_δ, given by (2.14), is a Λ-Lipschitz domain. Here, for simplicity, we assume the latter to be true.

2.3 Medium dependent weight function

Given $\varepsilon > 0$ and $v \in H^1(\Omega)$, with $\nabla v \in L^\infty(\Omega)$, we define the weight function $\mu_\varepsilon[v]$ as

$$\mu_\varepsilon[v](x) = \hat{\mu}_\varepsilon(|\nabla v(x)|), \qquad x \in \Omega, \tag{2.16}$$

where $\hat{\mu}_\varepsilon : [0, \infty) \to \mathbb{R}$ is a non-increasing function that satisfies

$$\hat{\mu}_\varepsilon(0) = \varepsilon^{-1}, \qquad 0 < \hat{\mu}_\varepsilon(t), \quad t\hat{\mu}_\varepsilon(t) \le 1, \quad t \ge 0, \tag{2.17}$$

and

$$\exists C > 0, \text{ s.t. for every sufficiently large } t,\ C \le t\hat{\mu}_\varepsilon(t). \tag{2.18}$$

In particular, for $\hat{\mu}_\varepsilon(t) = 1/(t^q + \varepsilon^q)^{1/q}$ and $\hat{\mu}_\varepsilon(t) = 1/\max(t, \varepsilon)$, as in (2.2) and (2.3), respectively, (2.17)-(2.18) hold for any $C < 1$. From (2.17), we immediately conclude that

$$\mu_\varepsilon[v](x)|\nabla v(x)| \le 1, \qquad \text{a.e. } x \in \Omega, \tag{2.19}$$

and

$$0 < \hat{\mu}_\varepsilon(\|\nabla v\|_{L^\infty(\Omega)}) \le \mu_\varepsilon[v](x) \qquad \text{a.e. } x \in \Omega. \tag{2.20}$$

2.4 Boundary value problems

Let $\mathcal{V}^\delta$ be a closed subspace of $H^1(\Omega)$, and $\mathcal{V}^\delta_0 = \mathcal{V}^\delta \cap H^1_0(\Omega)$. For sufficiently small and fixed $\delta, \varepsilon > 0$, the operator $L_\varepsilon[u_\delta]$ in (2.1) is uniformly elliptic in Ω [5]. Thus, it admits in $\mathcal{V}^\delta_0$ a (possibly finite) non-decreasing sequence $\{\lambda_k\}_{k\ge1}$ of positive eigenvalues with each repeated according to its multiplicity with corresponding eigenfunctions $\{\varphi_k\}_{k\ge1}$ which form an L^2-orthonormal basis of $\mathcal{V}^\delta_0$. In addition, we denote by $\varphi_0 \in \mathcal{V}^\delta$ the $L_\varepsilon[u_\delta]$-lifting of the boundary data of u_δ into Ω. More precisely, we let $\varphi_0 \in \mathcal{V}^\delta$ satisfy

$$L_\varepsilon[u_\delta]\varphi_0 = 0 \quad \text{in } \Omega, \qquad \varphi_0 = u_\delta \quad \text{on } \partial\Omega \tag{2.21}$$

in $\mathcal{V}_0^\delta$, and for $k \geq 1$ we let $\varphi_k \in \mathcal{V}_0^\delta$, $\varphi_k \neq 0$ satisfy

$$L_\varepsilon[u_\delta]\varphi_k = \lambda_k \varphi_k \quad \text{in } \Omega, \qquad \varphi_k = 0 \quad \text{on } \partial\Omega, \tag{2.22}$$

in $\mathcal{V}_0^\delta$. Clearly both (2.21) and (2.22) should be understood in a weak sense with respect to the bilinear form

$$B_{\varepsilon\delta}[w, v] = \langle \mu_\varepsilon[u_\delta]\nabla w, \nabla v \rangle\,. \tag{2.23}$$

Remark 2.3. Note that φ_k ($k \geq 0$) and λ_k ($k \geq 1$) depend on ε and u_δ, and thus on u and δ. For simplicity of notation, we do not indicate this dependency explicitly.

3 Error estimates

Since u_δ is an admissible approximation of u, as defined in Section 2.2, for every $\varepsilon > 0$ and every sufficiently small $\delta > 0$, we have [5]

$$B_{\varepsilon\delta}[u_\delta, u_\delta] \leq C, \qquad B_{\varepsilon\delta}[\varphi_k, \varphi_k] \leq C, \quad k = 0, 1, \ldots, K. \tag{3.1}$$

As a consequence, the gradients of φ_k, $k = 0, \ldots, K$, are small in D_δ [5, Theorem 5]. Heuristically, this implies that each φ_k is almost constant in regions where u is constant and thus we expect that u be well approximated in $\varphi_0 + \Phi_K^{\varepsilon,\delta}$, where

$$\Phi_K^{\varepsilon,\delta} = \text{span}\{\varphi_k\}_{k=1}^K. \tag{3.2}$$

Here, our goal is to rigorously prove this proposition.

More precisely, let $\Pi_K^\varepsilon[u_\delta]$ denote the standard orthogonal projection on $\Phi_K^{\varepsilon,\delta}$:

$$\Pi_K^\varepsilon[u_\delta] : L^2(\Omega) \to \Phi_K^{\varepsilon,\delta}, \qquad \langle v - \Pi_K^\varepsilon[u_\delta]v, \varphi \rangle = 0, \quad \forall\, \varphi \in \Phi_K^{\varepsilon,\delta}, \tag{3.3}$$

and let X_K be given by

$$X_K = \text{span}\{\chi_{A^k}\}_{k=1}^K = \text{span}\{\chi_{B^k}\}_{k=1}^K, \tag{3.4}$$

We shall show that every function $v \in u + X_K$ is well approximated in $\varphi_0 + \Phi_K^{\varepsilon,\delta}$ by its L^2-best approximation

$$Q_K^\varepsilon[u_\delta](v) = \varphi_0 + \Pi_K^\varepsilon[u_\delta](v - \varphi_0). \tag{3.5}$$

Similarly, we shall show that every $v \in X_K$ is well approximated by its orthogonal projection $\Pi_K^\varepsilon[u_\delta]v$ on $\Phi_K^{\varepsilon,\delta}$. The main result, given by Theorem 3.6, provides estimates of the L^2 errors in terms of ε and δ.

3.1 Preliminary results

From (2.20) with $v = u_\delta$, the monotonicity of $\hat{\mu}$, (2.11) and (2.18) we get

$$0 < C\delta \leq \mu_\varepsilon[u_\delta](x) \qquad \text{a.e. } x \in \Omega \tag{3.6}$$

for every sufficiently small δ, where the constant C may depend on u, but is independent of δ and ε. Since ∇u_δ vanishes in D_δ by (2.9), assumptions (2.16) and (2.17) on $\hat{\mu}_\varepsilon$ yield

$$\mu_\varepsilon[u_\delta](x) = \varepsilon^{-1} \qquad \text{a.e. } x \in D_\delta. \tag{3.7}$$

Together with the definition of $B_{\varepsilon\delta}[\cdot,\cdot]$ in (2.23), and (3.6) we obtain

$$\varepsilon^{-1}\|\nabla v\|^2_{L^2(D_\delta)} + C_1\delta\|\nabla v\|^2_{L^2(\mathcal{M}_\delta)} \leq B_{\varepsilon\delta}[v,v] \tag{3.8}$$

for every $\delta > 0$ sufficiently small and every $v \in H^1(\Omega)$. By substituting $v = \varphi_k$ in the above and using (3.1) we get

$$\varepsilon^{-1}\|\nabla \varphi_k\|^2_{L^2(D_\delta)} + C_1\delta\|\nabla \varphi_k\|^2_{L^2(\mathcal{M}_\delta)} \leq B_{\varepsilon\delta}[\varphi_k,\varphi_k] \leq C. \tag{3.9}$$

Next we employ (3.9) and PoincarÃľ-type inequalities to obtain L^2 estimates for φ_k in D_δ. To do that we require inequalities with constants independent of δ for the connected components of D_δ. We use Theorems 1 and 2 of [14] which yield the following: Let $p \geq 1$ and $\Lambda > 0$. There exists a constant $C > 0$ such that for every Λ-Lipschitz domain $W \subset \Omega$ and $v \in W^{1,p}(W)$,

$$\|v - \langle v\rangle_W\|_{L^2(W)} \leq C\|\nabla v\|_{L^2(W)}, \qquad \forall v \in W^{1,p}(W), \tag{3.10}$$

where $\langle f\rangle_W$ denotes the average of f over W,

$$\langle f\rangle_W = \frac{1}{\mathcal{L}(W)}\int_W f(x)dx, \tag{3.11}$$

with $\mathcal{L}(W)$ the Lebesgue measure of W. Moreover, if $\Gamma \subset \overline{\Omega}$ has positive $(d-1)$-dimensional Hausdorff measure, then for every Λ-Lipschitz domain $W \subset \Omega$, with $\Gamma \subset \partial W$, and $v \in W^{1,p}(W)$ satisfying $v = 0$ on Γ,

$$\|v\|_{L^p(W)} \leq C\|\nabla v\|_{L^p(W)}. \tag{3.12}$$

Corollary 3.1. *There exists a constant $C > 0$ such that for every $\varepsilon > 0$, $\delta > 0$ sufficiently small and $1 \leq j \leq K$,*

$$\|\varphi_0 - u^0\|^2_{L^2(E_\delta)} \leq C\varepsilon, \qquad \|\varphi_0 - \langle\varphi_0\rangle_{B^j_\delta}\|^2_{L^2(B^j_\delta)} \leq C\varepsilon \tag{3.13}$$

and

$$\|\varphi_k\|^2_{L^2(E_\delta)} \leq C\varepsilon, \qquad \|\varphi_k - \langle\varphi_k\rangle_{B^j_\delta}\|^2_{L^2(B^j_\delta)} \leq C\varepsilon, \qquad k = 1,\dots,K. \tag{3.14}$$

Proof. We show (3.13); the proof of (3.14) is similar. Fix $1 \leq m \leq M$. Then, for every sufficiently small δ, we have $\eta = \varphi_0 - u^0 \in H^1(E^m_\delta)$, with $\eta = 0$ on

$$\Gamma^m = \partial\Omega \cap \partial E^m_\delta.$$

As Γ^m contains an open set in the topology of $\partial\Omega$, its $(d-1)$-dimensional Hausdorff measure is positive. Since E^m_δ is Λ-Lipschitz, with Λ independent of δ, by PoincarÃľ (3.12), there exists $C_1 > 0$ such that

$$\|\eta\|_{L^2(E^m_\delta)} \leq C_1\|\nabla\eta\|_{L^2(E^m_\delta)}. \tag{3.15}$$

Now, we use the above combined with (3.9) and $\nabla u^0 = 0$ in E^m_δ, to obtain

$$\|\varphi_0 - u^0\|_{L^2(E^m_\delta)} = \|\eta\|_{L^2(E^m_\delta)} \leq C_1\|\nabla\varphi_0\|_{L^2(E^m_\delta)} \leq C_2\sqrt{\varepsilon}, \tag{3.16}$$

which proves the first estimate in (3.13), since E_δ is the disjoint (finite) union of E^m_δ. The proof of the second estimate in (3.13) is similar, but relies on (3.10) instead of (3.12); therefore, it is omitted here. □

While Corollary 3.1 provides L^2 estimates for φ_k in the connected components of D_δ, the following lemma provides L^2 estimates in $\mathcal{M}_\delta$. Especially, it yields that the contribution over $\mathcal{M}_\delta$ to the norm of φ_k is small. Note that to deduce this conclusion it is not enough to observe the volume of $\mathcal{M}_\delta$ is small, since φ_k themselves depend on δ.

Lemma 3.2. *There exists a positive constant C such that for every $k = 0, \dots, K$, and every sufficiently small $\varepsilon, \delta > 0$,*

$$\|\varphi_k\|^2_{L^2(\mathcal{M}_\delta)} \leq C\delta. \tag{3.17}$$

Proof. Here we show (3.17) only for $k = 1, \dots, K$. We include the case $k = 0$ here only for brevity. The proof for $k = 0$ is similar, however it requires Lemma 3.5. Thus, the correct order of our argument is (3.17) for $k = 1, \dots, K$, Lemma 3.3, Theorem 3.4, Lemma 3.5, and then (3.17) with $k = 0$.

Fix $1 \leq k \leq K$. Let $W = B^j$ for some $j = 1, \dots, K$ or $W = \Omega^m$ for some $m = 1, \dots, M$, let

$$U_\delta = \{x \in W : \operatorname{dist}(x, \partial W) < \delta\}. \tag{3.18}$$

By Theorem C.1 we have

$$\|\varphi_k\|^2_{L^2(U_\delta)} \leq C \left(\delta^2 \|\nabla\varphi_k\|^2_{L^2(U_\delta)} + \delta\|\varphi_k\|^2_{H^1(D_\delta)}\right). \tag{3.19}$$

By using $\|\varphi_k\|_{L^2(\Omega)} = 1$ and (3.9), we estimate the right hand side of (3.19) and thus for δ, ε sufficiently small obtain

$$\|\varphi_k\|^2_{L^2(U_\delta)} \leq C_1\delta\,(1 + \varepsilon) \leq C\delta. \tag{3.20}$$

Since $\mathcal{M}_\delta$ is a subset of the finite union of all $\overline{U_\delta}$, we obtain (3.17) which completes the proof. □

Following Corollary 3.1 and Lemma 3.2 we know that $\varphi_1, \dots, \varphi_K$ are approximately piecewise constant, and that the contributions over $\mathcal{M}_\delta$ to their norms are small. This implies that each φ_k is close to some function in X_K. The question now is if the converse is also true; i.e., can every function in X_K be well approximated in $\Phi_K^{\varepsilon,\delta}$? Since in every B^k_δ, $\varphi_1, \dots, \varphi_K$ are very close to their averages, this question reduces to the question of the linear independency of the vectors of their averages.

Lemma 3.3. *Let the matrix $\Sigma \in \mathbb{R}^{K\times K}$ be given by*

$$\Sigma = (\sigma_{kj}), \qquad \sigma_{kj} = \langle\varphi_j\rangle_{B^k_\delta}, \quad k, j = 1, \dots, K. \tag{3.21}$$

There exist constants $0 < C_1 \leq C_2$ such that for every sufficiently small δ and ε,

$$C_1|\beta| \leq |\Sigma\beta| \leq C_2|\beta|, \qquad \beta \in \mathbb{R}^K. \tag{3.22}$$

Proof. Since the upper estimate in (3.22) is simple, here we only show the lower estimate $C_1|\beta| \leq |\Sigma\beta|$, for some positive constant C_1 independent of β, ε, and δ. Let $\beta \in \mathbb{R}^K$ with $|\beta| = 1$ and $\varphi \in \Phi_K^{\varepsilon,\delta}$ be given by

$$\varphi = \sum_{j=1}^{K} \beta_j\varphi_j. \tag{3.23}$$

Then, we have

$$(\Sigma\beta)_k = \langle\varphi\rangle_{B_\delta^k}, \qquad k = 1, \dots, K, \tag{3.24}$$

where $(\Sigma\beta)_k$ denotes the k-th entry of $\Sigma\beta$. Since $\varphi_1, \dots, \varphi_K$ are orthonormal and $|\beta| = 1$, we get

$$1 = \|\varphi\|^2_{L^2(\Omega)} = \|\varphi\|^2_{L^2(E_\delta)} + \|\varphi\|^2_{L^2(\mathcal{M}_\delta)} + \sum_{k=1}^{K} \|\varphi\|^2_{L^2(B_\delta^k)}. \tag{3.25}$$

Due to (3.24), the function $\varphi - (\Sigma\beta)_k$ has zero average over B_δ^k and is, therefore, orthogonal to the constant in $L^2(B_\delta^k)$. Thus,

$$\|\varphi\|^2_{L^2(B_\delta^k)} = \|\varphi - (\Sigma\beta)_k\|^2_{L^2(B_\delta^k)} + \mathcal{L}(B_\delta^k)(\Sigma\beta)_k^2, \qquad k = 1, \dots, K. \tag{3.26}$$

By PoincarÃľ's inequality (3.10),

$$\|\varphi - (\Sigma\beta)_k\|^2_{L^2(B_\delta^k)} \le C\|\nabla\varphi\|^2_{L^2(B_\delta^k)} \tag{3.27}$$

and by the triangle inequality and (3.9), we have

$$\|\nabla\varphi\|_{L^2(B_\delta^k)} \le \sum_{j=1}^{K} |\beta_j| \|\nabla\varphi_j\|_{L^2(B_\delta^k)} \le C\sqrt{\varepsilon}. \tag{3.28}$$

We similarly apply (3.14) to estimate $\|\varphi\|_{L^2(E_\delta)}$ and use (3.17) with $k = 1, \dots, K$ to obtain

$$1 \le C(\varepsilon + \delta) + \sum_{k=1}^{K} \mathcal{L}(B_\delta^k)(\Sigma\beta)_k^2 \le C(\varepsilon + \delta) + \max_k \mathcal{L}(B^k)\,|\Sigma\beta|^2, \tag{3.29}$$

since $B_\delta^k \subset B^k$. Thus, for every δ and ε sufficiently small,

$$\widetilde{C} \le \max_k \mathcal{L}(B^k)\,|\Sigma\beta|^2 \tag{3.30}$$

which completes the proof. □

3.2 Main results

Next we show that if $\varepsilon, \delta > 0$ are sufficiently small, then the first eigenvalue of $L_\varepsilon[u_\delta]$ is bounded from below by a constant independent of ε, δ.

Theorem 3.4. *There exists a positive constant C such that for every $\varepsilon, \delta > 0$ sufficiently small and for every $v \in H_0^1(\Omega)$,*

$$C\|\nabla v\|_{L^1(\Omega)} \le \sqrt{B_{\varepsilon\delta}[v, v]}, \qquad C\|v\|^2_{L^2(\Omega)} \le B_{\varepsilon\delta}[v, v]. \tag{3.31}$$

In particular, the second estimate yields $\lambda_1 \ge C > 0$.

Proof. We begin by showing the first estimate of (3.31). Let $v \in H_0^1(\Omega)$. Using (3.8) we obtain

$$B_{\varepsilon\delta}[v,v] \geq C\delta\|\nabla v\|^2_{L^2(\mathcal{M}_\delta)} + \varepsilon^{-1}\|\nabla v\|^2_{L^2(D_\delta)}. \tag{3.32}$$

HÃűlder's inequality and Lemma 4 of [5] yield

$$\delta\|\nabla v\|^2_{L^2(\mathcal{M}_\delta)} \geq \frac{\delta}{\mathcal{L}(\mathcal{M}_\delta)}\|\nabla v\|^2_{L^1(\mathcal{M}_\delta)} \geq C\|\nabla v\|^2_{L^1(\mathcal{M}_\delta)}. \tag{3.33}$$

Similarly we use HÃűlder's inequality to estimate $\|\nabla v\|^2_{L^2(D_\delta)}$ from below by $C\|\nabla v\|^2_{L^1(D_\delta)}$ and thus for $\varepsilon > 0$ sufficiently small we get

$$B_{\varepsilon\delta}[v,v] \geq C_1\|\nabla v\|^2_{L^1(\Omega)}, \tag{3.34}$$

which is equivalent to the first estimate of (3.31).

Next we show the second estimate of (3.31). Since λ_1 is the smallest eigenvalue of (2.22) in $\mathcal{V}_0^\delta \subset H_0^1(\Omega)$, it is sufficient to show that for $\mathcal{V}_0^\delta = H_0^1(\Omega)$ there exists a positive constant C such that for every $\varepsilon, \delta > 0$ sufficiently small,

$$\lambda_1 = B_{\varepsilon\delta}[\varphi_1, \varphi_1] \geq C.$$

Substituting $v = \varphi_1$ into (3.34) yields

$$\lambda_1 = B_{\varepsilon\delta}[\varphi_1, \varphi_1] \geq C_1\|\nabla\varphi_1\|^2_{L^1(\Omega)} \tag{3.35}$$

Thus for $\varepsilon, \delta > 0$ sufficiently small, by PoincarÃľ's inequality (3.12) we get

$$\lambda_1 \geq C_1\|\nabla\varphi_1\|^2_{L^1(\Omega)} \geq C_2\|\varphi_1\|^2_{L^1(\Omega)}. \tag{3.36}$$

Therefore,

$$\sqrt{\lambda_1} \geq \sqrt{C_2}\sum_{k=1}^{K}\mathcal{L}(B_\delta^k)|\langle\varphi_1\rangle_{B_\delta}|. \tag{3.37}$$

As a consequence, for every $0 < \delta \leq \delta_0$, with δ_0 sufficiently small, we have

$$\sqrt{\lambda_1} \geq C_3 \min_k \mathcal{L}(B_{\delta_0}^k)\sum_{k=1}^{K}|\langle\varphi_1\rangle_{B_\delta^k}|, \tag{3.38}$$

where we have used that $B_\delta^k \supset B_{\delta_0}^k$. Finally, Lemma 3.3 yields

$$\sum_{k=1}^{K}|\langle\varphi_1\rangle_{B_\delta^k}| = |\Sigma e_1|_{\ell^1} \geq |\Sigma e_1| \geq C > 0, \tag{3.39}$$

where Σ is given by (3.21) and $e_1 = (1, 0, \ldots, 0)^T \in \mathbb{R}^K$, and thus $\lambda_1 \geq C > 0$. Since λ_1 is the minimum of the Rayleigh quotient in $H_0^1(\Omega) \setminus \{0\}$, we also have the second estimate of (3.31) which completes the proof. □

Estimate (3.13) bounds φ_0 in E_δ. Next we derive L^2 estimates for φ_0 in B_δ^k.

Lemma 3.5. *There exists a positive constant C, such that for each positive $\delta, \varepsilon > 0$ sufficiently small*

$$\|\varphi_0\|_{L^2(B_\delta^k)} \le C. \tag{3.40}$$

Proof. Let $\eta \in \mathcal{V}_0^\delta$ be given by $\eta = \varphi_0 - u_\delta$. Then, (2.21) implies

$$B_{\varepsilon\delta}[\varphi_0, \eta] = 0 \tag{3.41}$$

and thus using (3.1) we obtain

$$B_{\varepsilon\delta}[\eta, \eta] \le B_{\varepsilon\delta}[\eta, \eta] + B_{\varepsilon\delta}[\varphi_0, \varphi_0] = B_{\varepsilon\delta}[u_\delta, u_\delta] \le C. \tag{3.42}$$

Since $\eta = 0$ on $\partial\Omega$, we also have

$$\lambda_1 \|\eta\|^2_{L^2(\Omega)} \le B_{\varepsilon\delta}[\eta, \eta] \le C. \tag{3.43}$$

By Theorem 3.4, λ_1 is bounded from below by a positive constant independent of δ and ε. Therefore,

$$\|\varphi_0 - u_\delta\|_{L^2(B_\delta^k)} \le \|\varphi_0 - u_\delta\|_{L^2(\Omega)} = \|\eta\|_{L^2(\Omega)} \le C, \qquad k = 1, \ldots, K, \tag{3.44}$$

which yields (3.40) by the triangle inequality and (2.6). □

We can now prove the main results of this paper.

Theorem 3.6. *Let u, given by (2.4), be approximated by admissible u_δ as defined in Section 2.2, and let X_K be given by (3.4). For ε, δ positive, let $L_\varepsilon[\cdot]$ be given by (2.1) with $\mu_\varepsilon[\cdot]$ given by (2.16), let φ_0 satisfy (2.21), $\varphi_1, \ldots, \varphi_K$ satisfy (2.22), and $\Pi_K^\varepsilon[u_\delta]$ be the orthogonal projection on $\Phi_K^{\varepsilon,\delta}$, given by (3.3). If $v \in X_K$, then there exists a positive constant C such that for every sufficiently small ε, δ,*

$$\|v - \Pi_K^\varepsilon[u_\delta]v\|_{L^2(\Omega)} \le C\sqrt{\varepsilon + \delta}\,. \tag{3.45}$$

Similarly, if $v \in u + X_K$ and $Q_K^\varepsilon[u_\delta]$ is the least squares projection on $\varphi_0 + \Phi_K^{\varepsilon,\delta}$, given by (3.5), then for every sufficiently small ε, δ,

$$\left\|v - Q_K^\varepsilon[u_\delta](v)\right\|_{L^2(\Omega)} \le C\sqrt{\varepsilon + \delta}\,. \tag{3.46}$$

In particular, $v = \widetilde{u}$ satisfies (3.45), and $v = u$ and $v = u_0$ satisfy (3.46).

Remark 3.7. By the triangle inequality and the arguments of the proof of Theorem 3.6, for every $v \in X_K$ and $v_\delta \in L^2(\Omega)$, we have

$$\left\|v_\delta - \Pi_K^\varepsilon[u_\delta]v_\delta\right\|_{L^2(\Omega)} \le C\sqrt{\varepsilon + \delta} + \|v_\delta - v\|_{L^2(\Omega)}\,, \tag{3.47}$$

and, similarly, if $v \in u + X_K$ and $v_\delta \in L^2(\Omega)$, then

$$\left\|v_\delta - Q_K^\varepsilon[u_\delta](v_\delta)\right\|_{L^2(\Omega)} \le C\sqrt{\varepsilon + \delta} + \|v_\delta - v\|_{L^2(\Omega)}\,. \tag{3.48}$$

In particular, (3.47) is satisfied for $v = \widetilde{u}$ and $v_\delta = \widetilde{u}_\delta$, and (3.48) is satisfied for $v = u$ and $v_\delta = u_\delta$ and for $v = u^0$ and $v_\delta = u_\delta^0$.

Similarly to Corollary 6 of [5], we have the following:

Corollary 3.8. *1. If u_δ is the interpolation of u in a FE space V_δ as in Example 2.1, and either $\mathcal{V}^\delta = V_\delta$ or $\mathcal{V}^\delta = H^1(\Omega)$, then for every $\varepsilon, \delta > 0$ sufficiently small estimates* (3.45) *and* (3.46) *hold true.*

2. If u_δ is the mollification of u as in Example 2.2 and $\mathcal{V}^\delta = H^1(\Omega)$, then for every $\varepsilon, \delta > 0$ sufficiently small estimates (3.45) *and* (3.46) *hold true.*

Proof. This corollary is a direct result of Theorem 3.6 and examples 2.1 and 2.2. □

Proof of Theorem 3.6. Here, we only show (3.46); the proof of (3.45) is similar. We have

$$\left\|v - Q_K^\varepsilon[u_\delta](v)\right\|_{L^2(\Omega)} = \min_{\beta \in \mathbb{R}^K} \left\|(v - \varphi_0) - \sum_{k=1}^K \beta_k \varphi_k\right\|_{L^2(\Omega)}. \tag{3.49}$$

By Lemma 3.3 there exists a unique vector $\beta = (\beta_k) \in \mathbb{R}^K$ such that

$$\sum_{j=1}^K \beta_j \langle \varphi_j \rangle_{B_\delta^k} = \langle v - \varphi_0 \rangle_{B_\delta^k}, \tag{3.50}$$

and, moreover,

$$|\beta|^2 \le C_1 \sum_{k=1}^K \langle v - \varphi_0 \rangle_{B_\delta^k}^2 \tag{3.51}$$

for $C_1 > 0$ independent of ε and δ. Therefore, by Lemma 3.5, we have

$$|\beta| \le \sqrt{C_1} \left[\sum_{k=1}^K \|v - \varphi_0\|_{L^2(B_\delta^k)}^2\right]^{\frac{1}{2}} \le C \tag{3.52}$$

for $C > 0$ independent of ε, δ. For

$$\varphi = \varphi_0 + \widetilde{\varphi}, \qquad \widetilde{\varphi} = \sum_{k=1}^K \beta_k \varphi_k, \tag{3.53}$$

we have

$$\left\|v - Q_K^\varepsilon[u_\delta](v)\right\|_{L^2(\Omega)} \le \|v - \varphi\|_{L^2(\Omega)}. \tag{3.54}$$

By the triangle inequality, we get

$$\|v - \varphi\|_{L^2(\Omega)} \le \|v - \varphi\|_{L^2(E_\delta)} + \|v\|_{L^2(\mathcal{M}_\delta)} + \|\varphi\|_{L^2(\mathcal{M}_\delta)} + \sum_{k=1}^K \|v - \varphi\|_{L^2(B_\delta^k)}. \tag{3.55}$$

Next we estimate each of the terms on the right hand side. Since for every k, $B_\delta^k \cap E_\delta = \emptyset$, and $v = u$ in E_δ, we can estimate the first term as follows:

$$\|v - \varphi\|_{L^2(E_\delta)} \le \|u - \varphi_0\|_{L^2(E_\delta)} + \|\widetilde{\varphi}\|_{L^2(E_\delta)} \le C\sqrt{\varepsilon} \tag{3.56}$$

because of (3.52), (3.13) and (3.14). We estimate the second term as

$$\|v\|_{L^2(\mathcal{M}_\delta)} \leq \|v\|_{L^\infty(\mathcal{M}_\delta)}\sqrt{\mathcal{L}(\mathcal{M}_\delta)} \leq C\sqrt{\delta} \tag{3.57}$$

where we have used Lemma 4 in [5]. To estimate the third term on the right hand side of (3.55), we use Lemma 3.2. For each $k = 1, \dots, K$, we estimate $\|v-\varphi\|_{L^2(B^k_\delta)}$ as follows: Since β sovles (3.50), we have $\langle v-\varphi\rangle_{B^k_\delta} = 0$, which by the PoincarÃl' inequality (3.10) yields

$$\|v-\varphi\|_{L^2(B^k_\delta)} \leq C\|\nabla(v-\varphi)\|_{L^2(B^k_\delta)}. \tag{3.58}$$

Since $\nabla v = 0$ in B^k_δ, estimates (3.9) and (3.52) yield

$$\|v-\varphi\|_{L^2(B^k_\delta)} \leq C_1\|\nabla\varphi\|_{L^2(B^k_\delta)} \leq C_2\sqrt{\varepsilon}. \tag{3.59}$$

Finally, by combining the above, we obtain

$$\left\|v - Q^\varepsilon_K[u_\delta](v)\right\|_{L^2(\Omega)} \leq \|v-\varphi\|_{L^2(\Omega)} \leq C\sqrt{\varepsilon+\delta} \tag{3.60}$$

which completes the proof. □

4 Numerical examples

Here we present numerical examples which illustrate the main results of our analysis and, in particular, the remarkable accuracy of AS decompositions for piecewise constant media[1]. First, we consider media comprised of a constant background and a single characteristic function. Secondly we consider a medium which consists of an inhomogeneous background comprised of five sets Ω^m, $m = 1, \dots, 5$, and four interior inclusions A^k, $k = 1, \dots, 4$ (see Section 2.1). In the third example, we consider a medium which consists of four adjacent squares in a constant background. Since the boundaries of the squares are not mutually disjoint, this example is not covered by our theory. Next we apply the AS decomposition to a polygonal approximation of the map of Switzerland with its 26 cantons. Finally, we consider the well-known Marmousi model from seismic imaging.

In all examples the domain $\Omega \subset \mathbb{R}^2$ is rectangluar and we use a regular, uniform triangular mesh $\mathcal{T}_h$ whose vertices lie on an equidistant Cartesian grid of size $h > 0$. We let $\mathcal{V}^\delta \subset H^1(\Omega)$, with $\delta = h$, be the standard $\mathcal{P}^1$ FE space of continuous piecewise linear functions and set $\mathcal{V}^\delta_0 = \mathcal{V}^\delta \cap H^1_0$. For piecewise constant u, we let u_δ denote the H^1-conforming (continuous) interpolation of u in the FE space $\mathcal{V}^\delta$.

We consider decompositions associated with $L_\varepsilon[u_\delta]$ given by (2.1) with $\mu_\varepsilon[\cdot]$ of the form (2.2) with $q = 2$. We compute the approximation of the background φ_0 and the first few eigenfunctions φ_k of $L_\varepsilon[u_\delta]$ by numerically solving (2.21) and (2.22) using the Galerkin FE method. The discretization of (2.22) leads to a generalized eigenvalue problem

$$\mathrm{A}\varphi_k = \lambda_k \mathrm{M}\varphi_k \quad \text{for} \quad k = 1, \dots, K, \tag{4.1}$$

where the stiffness matrix A corresponds to the discretization of $L_\varepsilon[u_\delta]$ and M is the mass matrix. We solve (4.1) numerically using the MATLAB function `eigs`.

[1] We will use the term *medium* for functions from $\Omega \subset \mathbb{R}^2$ into $\mathbb{R}$.

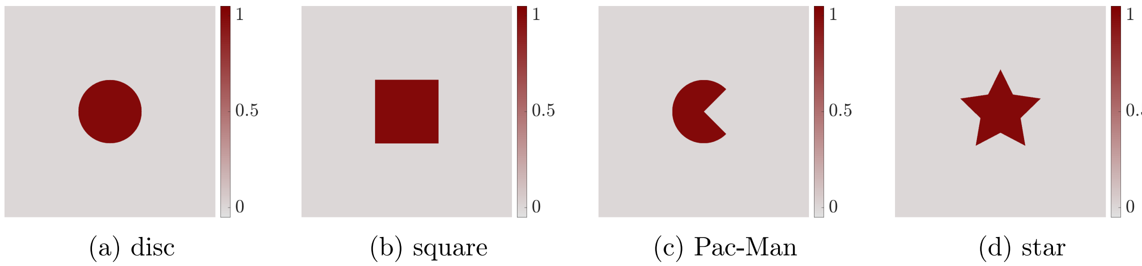

Figure 2: Four simple shapes. The exact medium u (or u_δ) consists of a single characteristic function χ_{A^1} and vanishing u^0.

Once we have obtained $\varphi_0 \in \mathcal{V}^\delta$ and $\varphi_k \in \mathcal{V}_0^\delta$ for $k = 1, \ldots, K$, we can compute the projections $\Pi_K^\varepsilon[u_\delta]$ and $Q_K^\varepsilon[u_\delta]$ given by (3.3) and (3.5). Since $\{\varphi_k\}_{k=1}^K$ are computed numerically, they satisfy $\langle \varphi_k, \varphi_j \rangle = \delta_{kj}$ only up to a small error. This slight loss of orthonormality causes small errors when computing the projection $\Pi_K^\varepsilon[u_\delta]$ directly from the Fourier expansion

$$\Pi_K^\varepsilon[u_\delta]v = \sum_{k=1}^K \langle \varphi_k, v\rangle \, \varphi_k.$$

To avoid these errors, we instead compute $\Pi_K^\varepsilon[u_\delta]v$ by solving the K-dimensional least squares problem

$$\Pi_K^\varepsilon[u_\delta]v = \operatorname*{argmin}_{w \in \Phi_K^{\varepsilon,\delta}} \|v - w\|_{L^2(\Omega)}, \qquad \Phi_K^{\varepsilon,\delta} = \operatorname{span}\{\varphi_k\}_{k=1}^K.$$

When validating the conclusion of Theorem 3.6 and its corollary in Remark 3.7, we shall focus on two types of errors

$$\|u - Q_K^\varepsilon[u_\delta](u)\|_{L^2(\Omega)} \qquad \text{and} \qquad \|u_\delta - Q_K^\varepsilon[u_\delta](u_\delta)\|_{L^2(\Omega)}; \tag{4.2}$$

the first measures the misfit to the true medium u whereas the second measures the misfit to the continuous interpolant u_δ. Note that in both cases the same AS basis is used. Computing these expressions requires the evaluation of L^2 inner products. As the functions participating in the expression on the right lie in the FE space $\mathcal{V}^\delta$, we can evaluate the needed integrals exactly. In contrast, the expression on the left includes inner products involving a piecewise constant function whose discontinuities are, in general, not aligned with the mesh. Thus, to evaluate the integrals for the error on the left in (4.2), we use a numerical quadrature rule from ACM TOMS algorithm #584 [15] with degree of precision of 8 and 19 quadrature points.

In principle, $\varepsilon > 0$ should be as small as possible, while sufficiently large so that the matrix A is well-conditioned. Unless specified otherwise, we always use $\varepsilon = 10^{-8}$.

4.1 Four simple shapes

We consider the four 2-dimensional piecewise constant media $u : \Omega \to \mathbb{R}$, in $\Omega = (0,1)^2$, shown in Fig. 2. All four vanish on the boundary $\partial\Omega$ and correspond to the characteristic function

$$u(x) = \widetilde{u}(x) = \chi_{A^1}(x), \quad x \in \Omega \tag{4.3}$$

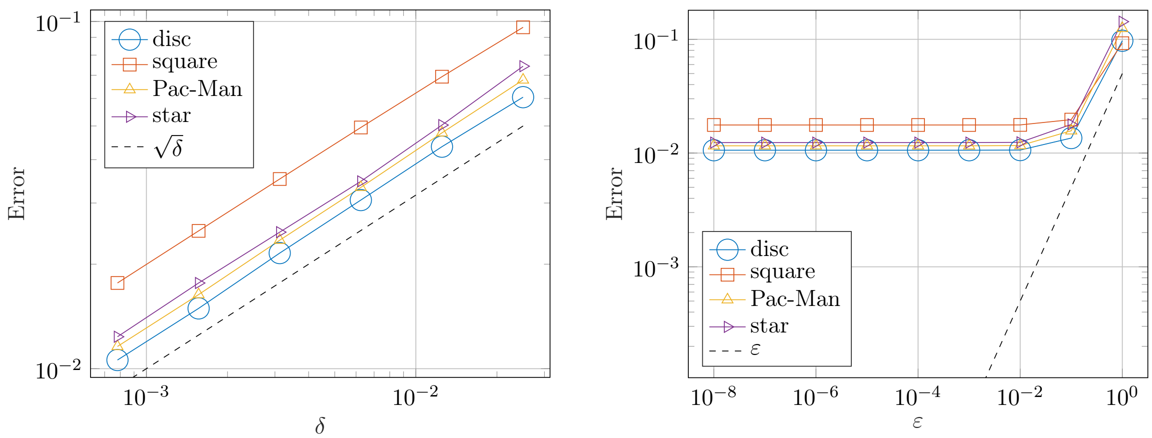

Figure 3: Four simple shapes. The error $\|u - \Pi_1^\varepsilon[u_\delta](u)\|_{L^2(\Omega)}$. Left: the error as a function of δ for fixed $\varepsilon = 10^{-8}$. Right: the error as a function of ε for fixed mesh-size $\delta = 0.05/2^6$.

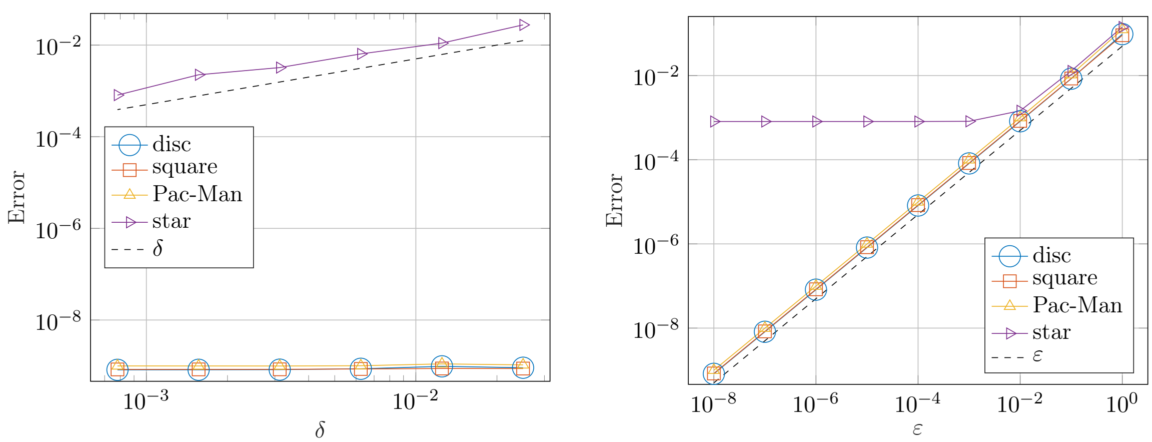

Figure 4: Four simple shapes. The error $\|u_\delta - \Pi_1^\varepsilon[u_\delta](u_\delta)\|_{L^2(\Omega)}$. Left: the error as a function of δ for fixed $\varepsilon = 10^{-8}$. Right: the error as a function of ε for fixed mesh-size $\delta = 0.05/2^6$.

of a Lipschitz domain and are therefore covered by our analysis. The sets are chosen purposely with different geometric properties: the disc is convex with a smooth boundary; the square is convex, but its boundary is only piecewise smooth; the Pac-Man and the star are both non-convex with piecewise smooth boundaries.

In Figure 3, we show the error $\|u - \Pi_1^\varepsilon[u_\delta](u)\|_{L^2(\Omega)}$. The left frame shows the error for varying mesh-size δ but fixed $\varepsilon = 10^{-8}$. For all four shapes, the error decays as $\mathcal{O}(\sqrt{\delta})$, as proved in Theorem 3.6. The right frame of Figure 3 shows the error $\|u - \Pi_1^\varepsilon[u_\delta](u)\|_{L^2(\Omega)}$ for varying ε on the fixed finest mesh, i.e., with smallest δ. The error initially decreases with ε but then levels off at about 10^{-2}, at which point it can only be improved by further refining the mesh.

To eliminate the interpolation error and thereby illustrate the estimates of Remark 3.7, we show in Figure 4 the projection error $\|u_\delta - \Pi_1^\varepsilon[u_\delta](u_\delta)\|_{L^2(\Omega)}$. On the left, we show the approximation error for varying δ, with $\varepsilon = 10^{-8}$ fixed: The projections of the disc, the square, and the Pac-Man in the AS basis are remarkably good, with errors at about 10^{-9}.

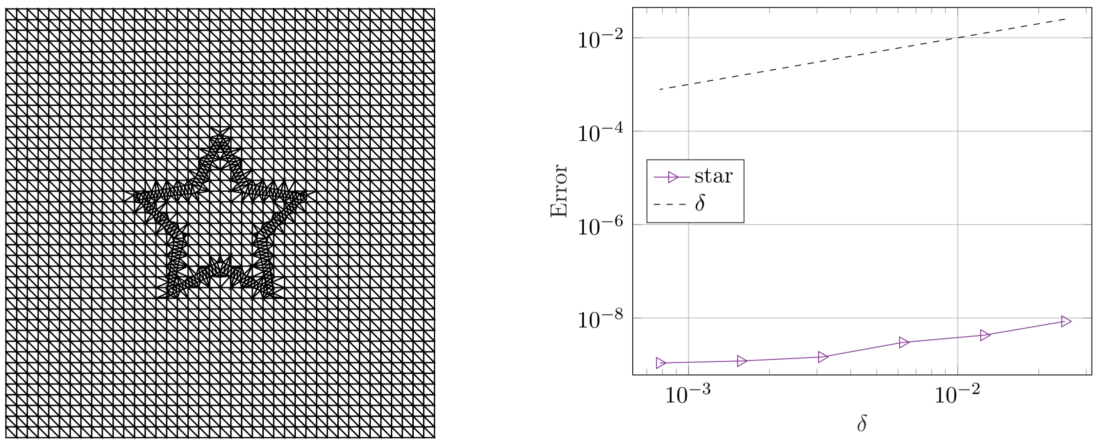

Figure 5: Four simple shapes. Left: The aligned mesh for the star-shaped medium with $\delta = 0.05/2^2$. Right: the error $\|u_\delta - \Pi_1^\varepsilon[u_\delta](u_\delta)\|_{L^2(\Omega)}$ for mesh-sizes $\delta = 0.05/2^m$, $m = 1, \ldots, 6$, and fixed $\varepsilon = 10^{-8}$.

For these cases, the projection of each u_δ (hence the first eigenfunction φ_1 of $L_\varepsilon[u_\delta]$) essentially coincides with u_δ itself. In contrast, the error for the star is larger, though it decays at a rate of $\mathcal{O}(\delta)$, still faster than the upper estimate of $\mathcal{O}(\sqrt{\delta})$ in Remark 3.7. In all cases, the errors here are significantly smaller than those in the left frame of Figure 3, indicating that the errors in Figure 3 are mainly due to interpolating u in $\mathcal{V}^\delta$.

The error $\|u_\delta - \Pi_1^\varepsilon[u_\delta](u_\delta)\|_{L^2(\Omega)}$ for varying ε and fixed δ is shown in the right frame of Figure 4. Here we observe a decay rate of $\mathcal{O}(\varepsilon)$, which is also faster than the upper estimate in Remark 3.7. Here, for all shapes but the star, the error decreases with ε down to about 10^{-9}. In contrast, the error for the star levels off at about 10^{-3}.

The significant difference in the behavior of the error for the star compared to the other shapes, shown in Figure 4, is due to the geometry of the discontinuities in the media and the mesh. Indeed, if we repeat the experiment for the star but with a locally adapted mesh aligned with the star's geometry, as shown in Figure 5, the error $\|u_\delta - \Pi_1^\varepsilon[u_\delta](u_\delta)\|_{L^2(\Omega)}$ also drops below 10^{-8}. Note that while δ is smaller in this test than it is in the tests shown in Figure 4, this reduction by itself is not sufficient to explain the difference in the errors between figures 4 and 5, which is of about 6 orders of magnitude.

4.2 Nonuniform background

Next we consider a medium u with non-constant background u^0. We let $u : \Omega \to \mathbb{R}$ be the medium shown in frame (a) of Fig. 6, and $\Omega = (0,1)^2$. Here u admits a decomposition (2.4), (2.5) with $M = 5$ and $K = 4$. Figure 6 also shows the approximation φ_0 of the background and the first four eigenfunctions $\varphi_1, \ldots, \varphi_4$ of $L_\varepsilon[u_\delta]$.

Figure 7 (left) shows the error $\|u - Q_K^\varepsilon[u_\delta](u)\|_{L^2(\Omega)}$ with $K = 4$, for six different meshes with $\delta = 0.05/2^m$, $m = 1, \ldots, 6$. Here we observe an error decay of $\mathcal{O}(\sqrt{\delta})$, consistent with our theoretical estimates. The right frame of Figure 7 shows the error $\|u_\delta - Q_K^\varepsilon[u_\delta](u_\delta)\|_{L^2(\Omega)}$ with $K = 4$, as a function of ε with fixed $\delta = 0.05/2^6$. Again, we observe a convergence rate of $\mathcal{O}(\varepsilon)$, faster than the $\mathcal{O}(\sqrt{\varepsilon})$ rate proved in Remark 3.7.

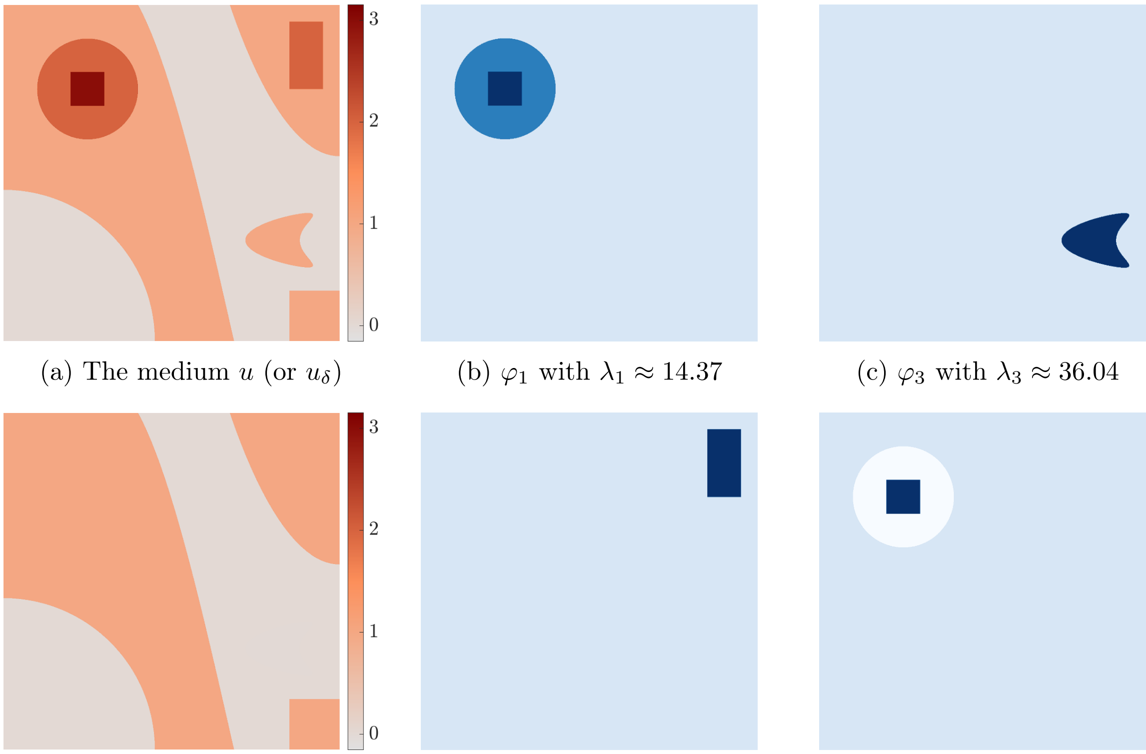

(a) The medium u (or u_δ) (b) φ_1 with $\lambda_1 \approx 14.37$ (c) φ_3 with $\lambda_3 \approx 36.04$

(d) φ_0 (e) φ_2 with $\lambda_2 \approx 29.88$ (f) φ_4 with $\lambda_4 \approx 50.48$

Figure 6: Nonuniform background. The exact medium u with its background φ_0 and first four eigenpairs (λ_i, φ_i), $i = 1, \ldots, 4$.

4.3 Four adjacent Squares

Let Ω be the unit square $\Omega = (0, 1)^2$ and

$$u(x) = \sum_{k=1}^{4} \alpha_k \chi_{A^k}(x), \quad x \in \Omega, \tag{4.4}$$

with $\alpha_k = k$, for $k = 1, \ldots, 4$, the piecewise constant medium shown in Fig. 8. Since the boundaries ∂A^k of the squares A^k are not mutually disjoint, this example is not covered by our analysis. However, we may still compute the AS approximation and measure the approximation error.

In Figure 9 we still observe errors of $\mathcal{O}(\sqrt{\delta})$, consistent with our theoretical estimates. Again, the error with respect to ε decays with a rate of $\mathcal{O}(\varepsilon)$, as seen in Figure 9.

4.4 Map of Switzerland

Here we consider the polygonal approximation of the map of Switzerland with its $K = 26$ cantons, shown in frame (a) of Figure 10, where each canton admits a constant value. The data of the map are given on a discrete rectangular pixel based 1563 px $\times$ 1002 px grid with grid-size $\delta = 1$ px. We interpolate the data to obtain $u_\delta \in \mathcal{V}_0^\delta$, and compute the first $K = 26$

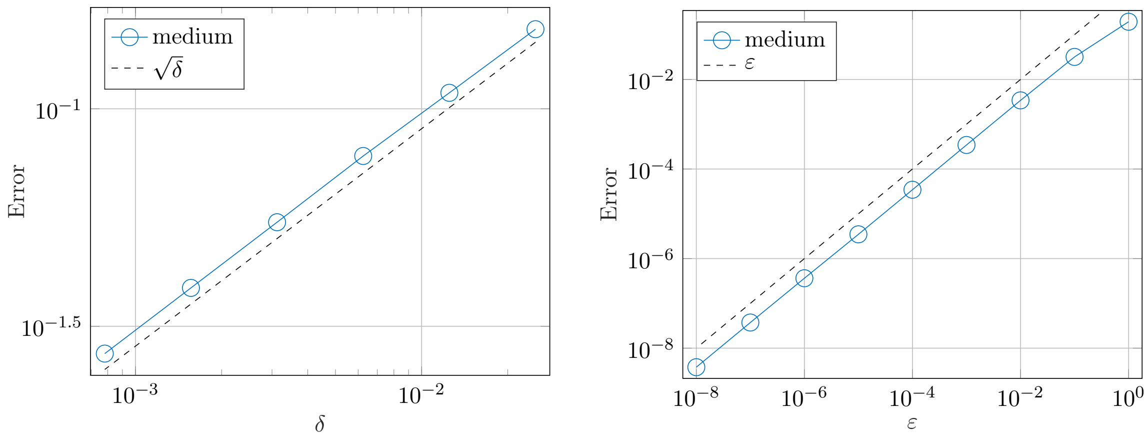

Figure 7: Nonuniform background. Left: the error $\|u - Q_4^\varepsilon[u_\delta](u)\|_{L^2(\Omega)}$ for mesh-sizes $\delta = 0.05/2^m$, $m = 1, \ldots, 6$, and fixed $\varepsilon = 10^{-8}$. Right: the error $\|u_\delta - Q_4^\varepsilon[u_\delta](u_\delta)\|_{L^2(\Omega)}$ for $\varepsilon = 10^{-m}$, $m = 0, \ldots, 8$, and fixed mesh-size $\delta = 0.05/2^6$.

eigenfunctions, $\varphi_1, \ldots, \varphi_K$ of $L_\varepsilon[u_\delta]$; frames (c), (d) and (e) of Figure 10 show three of the eigenfunctions.

Although a single eigenfunction does not necessarily correspond to any particular canton, we may still represent each canton in $\Phi_{26}^{\varepsilon,\delta} = \operatorname{span}\{\varphi_k\}_{k=1}^{26}$. If u^{c} is the characteristic function for a canton shown in the map in Figure 10, and u_δ^{c} is its continuous (piecewise linear) interpolant in $\mathcal{V}^\delta$, we can use the AS basis $\{\varphi_k\}_{k=1}^K$ to approximate u_δ^{c} as

$$u_\delta^{\mathrm{c}} \approx \Pi_K^\varepsilon[u_\delta]\, u_\delta^{\mathrm{c}} = \sum_{k=1}^{K} \beta_k \varphi_k,$$

with $K = 26$. In Figure 11 we show the approximations for the cantons of Bern, Grisons, and St. Gallen in $\Phi_{26}^{\varepsilon,\delta} = \operatorname{span}\{\varphi_k\}_{k=1}^K$. These reconstructions approximate very well the exact cantons in Figure 10.

4.5 The Marmousi model

As a last example we consider the subsurface model of the P-wave velocity of the AGL elastic Marmousi model shown in Figure 12, see [16, 17]. The data of the model is given as nodal values on a discrete rectangular mesh representing a 17 km × 3.5 km area. We interpolate the data in $\mathcal{V}^\delta$ with $\delta = 2.5\,\mathrm{m}$ to obtain u_δ. Next, we compute the background $\varphi_0 \in \mathcal{V}^\delta$ as well as the first 100 eigenfunctions of the operator $L_\varepsilon[u_\delta]$.

Remarkably, the background φ_0 already yields a good approximation of the model with a relative error of

$$\frac{\|u_\delta - Q_0^\varepsilon[u_\delta](u_\delta)\|_{L^2(\Omega)}}{\|u_\delta\|_{L^2(\Omega)}} = \frac{\|u_\delta - \varphi_0\|_{L^2(\Omega)}}{\|u_\delta\|_{L^2(\Omega)}} \approx 12.8\%,$$

probably because many of the internal layers in the model reach the boundary and thus can be recovered by φ_0. In contrast, the eigenfunctions φ_k ($k \geq 1$) account for variations of the medium in the interior of the domain. Here, the additional contribution of the first

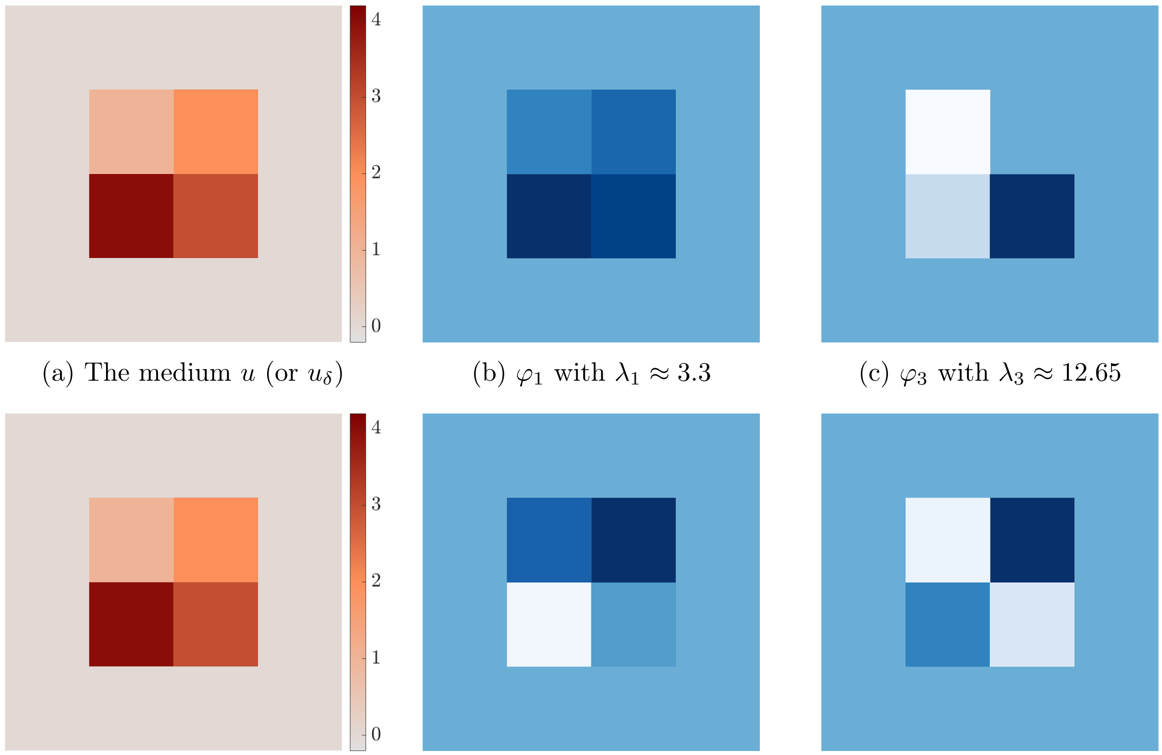

(a) The medium u (or u_δ) (b) φ_1 with $\lambda_1 \approx 3.3$ (c) φ_3 with $\lambda_3 \approx 12.65$

(d) $\Pi_4^\varepsilon[u_\delta]u_\delta$ (e) φ_2 with $\lambda_2 \approx 8.88$ (f) φ_4 with $\lambda_4 \approx 18.37$

Figure 8: Adjacent squares. The medium u and the first four eigenfunctions φ_k, $k = 1, \ldots, 4$, of the operator $L_\varepsilon[u_\delta]$, together with its AS decomposition $\Pi_4^\varepsilon[u_\delta](u_\delta)$ computed on a mesh with $\delta = 0.05/2^6$.

$K = 100$ eigenfunctions to the approximation further reduces the relative error to $\|u_\delta - Q_K^\varepsilon[u_\delta](u_\delta)\|_{L^2(\Omega)}/\|u_\delta\|_{L^2(\Omega)} \approx 3.8\%$.

Acknowledgments. We thank Giovanni Alberti and Gianluca Crippa for their useful comments and suggestions regarding Appendix B.

A Admissible approximations

Let u, as in Section 2.1, be approximated by u_δ obtained by a linear method, $u_\delta = \mathcal{I}_\delta u$. We assume that for every $k = 1, \ldots, K$ and $m = 1, \ldots, M$ the approximations $\mathcal{I}_\delta \chi_{A^k} \in \mathcal{V}_0^\delta$ of χ_{A^k} and $\mathcal{I}_\delta \chi_{\Omega^m} \in \mathcal{V}^\delta$ of χ_{Ω^m} satisfy

$$\lim_{\delta \to 0} \|\mathcal{I}_\delta \chi_{A^k} - \chi_{A^k}\|_{L^2(\Omega)} = 0, \qquad \lim_{\delta \to 0} \|\mathcal{I}_\delta \chi_{\Omega^m} - \chi_{\Omega^m}\|_{L^2(\Omega)} = 0. \tag{A.1}$$

For each $\delta > 0$, the H^1-regular approximation u_δ of u is thus given by

$$u_\delta \;=\; u_\delta^0 + \widetilde{u}_\delta, \tag{A.2}$$

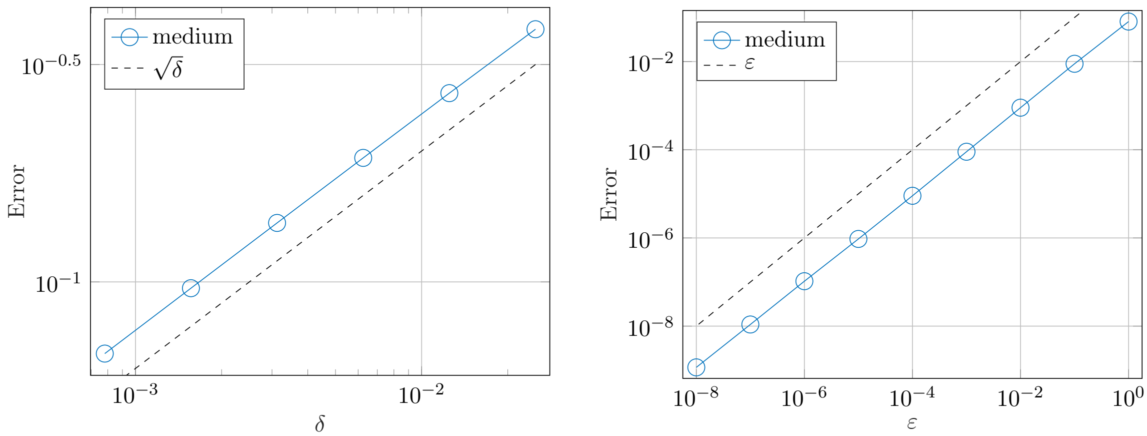

Figure 9: Adjacent squares. Left: the error $\|u - \Pi_4^\varepsilon[u_\delta](u)\|_{L^2(\Omega)}$ for mesh-sizes $\delta = 0.05/2^m$, $m = 1, \dots, 6$, and fixed $\varepsilon = 10^{-8}$. Right: the error $\|u_\delta - \Pi_4^\varepsilon[u_\delta](u_\delta)\|_{L^2(\Omega)}$ for $\varepsilon = 10^{-m}$, $m = 0, \dots, 8$, and fixed mesh-size $\delta = 0.05/2^6$;

where

$$u_\delta^0 = \mathcal{I}_\delta u^0 = \sum_{m=1}^{M} \omega_m \, \mathcal{I}_\delta \chi_{\Omega^m} \in \mathcal{V}^\delta, \qquad \widetilde{u}_\delta = \mathcal{I}_\delta \widetilde{u} = \sum_{k=1}^{K} \alpha_k \, \mathcal{I}_\delta \chi_{A^k} \in \mathcal{V}_0^\delta. \tag{A.3}$$

Next we introduce two assumptions regarding u_δ. For this we require additional notation. Let

$$S_\delta = \bigcup_{m=1}^{M} \big\{ x \in \Omega \,|\; \operatorname{dist}(x, \partial\Omega^m \cap \Omega) < \delta \big\}, \tag{A.4}$$

and, similarly,

$$U_\delta^k = \big\{ x \in \Omega \,|\; \operatorname{dist}(x, \partial A^k) < \delta \big\}. \tag{A.5}$$

Assumption 1. *For each $m = 1, \dots, M$,*

$$\nabla(\mathcal{I}_\delta \chi_{\Omega^m}) \in L^\infty(\Omega), \quad \operatorname{supp}\big(\nabla(\mathcal{I}_\delta \chi_{\Omega^m})\big) \subset \overline{S_\delta}, \tag{A.6a}$$

and for each $k = 1, \dots, K$,

$$\nabla(\mathcal{I}_\delta \chi_{A^k}) \in L^\infty(\Omega), \quad \operatorname{supp}\big(\nabla(\mathcal{I}_\delta \chi_{A^k})\big) \subset \overline{U_\delta^k}. \tag{A.6b}$$

Assumption 2. *There exists a constant C such that for every $\delta > 0$ sufficiently small, each of the functions $\chi_\delta = \mathcal{I}_\delta \chi_{\Omega^m}$, $m = 1, \dots, M$, and $\chi_\delta = \mathcal{I}_\delta \chi_{A^k}$, $k = 1, \dots, K$, satisfies*

$$\delta \|\nabla \chi_\delta\|_{L^\infty(\Omega)} \;\le\; C. \tag{A.7}$$

We say that u_δ is an admissible approximation of u, or that the method $\mathcal{I}_\delta$ is admissible if the conditions of this section are satisfied.

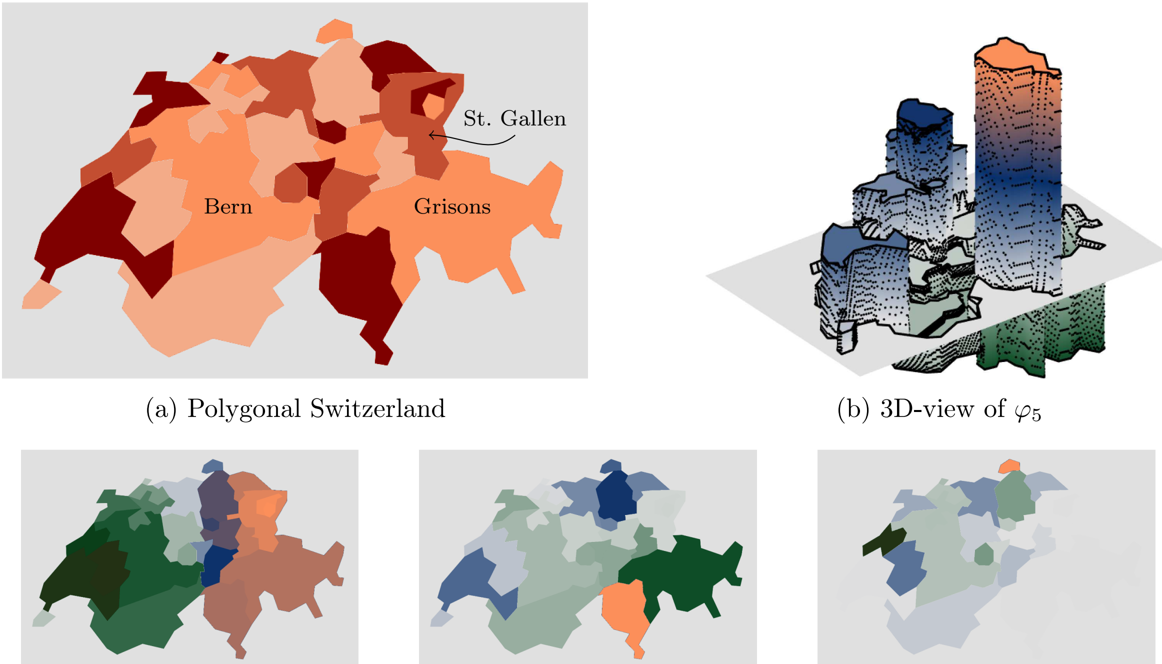

(a) Polygonal Switzerland

(b) 3D-view of φ_5

(c) φ_2 with $\lambda_2 \approx 28.75$

(d) φ_5 with $\lambda_5 \approx 85.03$

(e) φ_{15} with $\lambda_{15} \approx 217.59$

Figure 10: Polygonal approximation of the map of Switzerland u_δ and its 26 cantons (top left), together with three eigenfunctions φ_k, $k = 2, 5, 15$, of the operator $L_\varepsilon[u_\delta]$.

B Level sets of distance functions

In the following, for $p_1, p_2 \in \mathbb{R}^d$, $\operatorname{dist}(p_1, p_2)$ denotes the Euclidean distance

$$\operatorname{dist}(p_1, p_2) = |p_1 - p_2|$$

between p_1 and p_2. Here we prove the following theorem:

Theorem B.1. *If $A \subset \mathbb{R}^d$ is a Λ-Lipschitz domain with bounded boundary, and $\delta > 0$ sufficiently small, then A_δ given by*

$$A_\delta = \{x \in A : \operatorname{dist}(x, \partial A) > \delta\} \tag{B.1}$$

is also Λ-Lipschitz.

We say that a domain $A \subset \mathbb{R}^d$ with bounded boundary ∂A is Λ-Lipschitz, if locally ∂A coincides with the graph of a Λ-Lipschitz function f with A lying above f [18]. As a preliminary result we first show in Theorem B.6 of Section B.1 a similar result for a set lying above the graph of a Lipschitz function.

B.1 Distance functions for Lipschitz graphs

Let $\hat{\mathcal{B}} \subset \mathbb{R}^{d-1}$ be a ball of radius R, $f : \hat{\mathcal{B}} \to \mathbb{R}$ Λ-Lipschitz, $\widehat{F}$ the graph of f in $\hat{\mathcal{B}}$, $\mathcal{B} \subset \hat{\mathcal{B}}$ a ball of radius $r < R$ concentric with $\hat{\mathcal{B}}$, and

$$G(\delta) = \left\{p = (x, y) : \ x \in \mathcal{B},\ y > f(x),\ \operatorname{dist}(p, \widehat{F}) = \delta\right\}. \tag{B.2}$$

(a) Canton of Bern (b) Canton of Grisons (c) Canton of St. Gallen

Figure 11: Map of Switzerland. Three cantons approximated in the truncated AS basis $\{\varphi_k\}_{k=1}^K$ with $K = 26$.

The setup is illustrated in the left frame of Figure 13. Here we show that $G(\delta)$ is the graph of a Λ-Lipschitz function $g : \mathcal{B} \to \mathbb{R}$.

For $p \in \mathbb{R}^d$, we let $\mathcal{C}_p$ denote the open (two-sided) infinite cone,

$$\mathcal{C}_p = p + \mathcal{C}_0, \qquad \mathcal{C}_0 = \big\{(x, y) \in \mathbb{R}^{d-1} \times \mathbb{R} : \ |y| > \Lambda |x|\big\}.$$

We shall use that a function $g : \mathcal{B} \to \mathbb{R}$ is Λ-Lipschitz if and only if for every point p in its graph, graph(g), we have $\mathcal{C}_p \cap \text{graph}(g) = \emptyset$.

First we show that for every $x \in \mathcal{B}$ and $y > f(x)$ sufficiently large, the distance of (x, y) to $\widehat{F}$ is greater than δ.

Proposition B.2. *If $x \in \mathcal{B}$ and $y > f(x) + \Lambda_0\delta$, with $\Lambda_0 = \sqrt{1 + \Lambda^2}$, then*

$$\text{dist}((x, y), \widehat{F}) > \delta; \tag{B.3}$$

especially $(x, y) \notin G(\delta)$.

Proof. Fix $x \in \mathcal{B}$ and $h > h_0 = \Lambda_0\delta$. We show that $p = (x, f(x) + h)$ satisfies $\text{dist}(p, \widehat{F}) > \delta$. If $\Lambda = 0$, then f is constant and the conclusion is clear. Suppose $\Lambda > 0$, and let $\hat{x} \in \hat{\mathcal{B}}$, $\hat{p} = (\hat{x}, f(\hat{x}))$, and $\tau = |f(x) - f(\hat{x})|/\Lambda$. Then,

$$\begin{aligned}
\text{dist}(p, \hat{p})^2 &= |x - \hat{x}|^2 + (f(x) + h - f(\hat{x}))^2 \\
&\geq \frac{1 + \Lambda^2}{\Lambda^2} |f(x) - f(\hat{x})|^2 - 2h|f(x) - f(\hat{x})| + h^2 \\
&= \left(1 + \Lambda^2\right) \tau^2 - 2h\Lambda\tau + h^2 =: \psi(\tau).
\end{aligned} \tag{B.4}$$

Since the minimum of ψ is achieved in

$$\tau_* = \frac{h\Lambda}{1 + \Lambda^2}, \tag{B.5}$$

we have

$$\text{dist}(p, \hat{p})^2 \geq \psi(\tau_*) = h^2 \left(1 - \frac{\Lambda^2}{1 + \Lambda^2}\right) = \frac{h^2}{1 + \Lambda^2} > \frac{(1 + \Lambda^2)\delta^2}{1 + \Lambda^2} = \delta^2 \tag{B.6}$$

which yields the conclusion. □

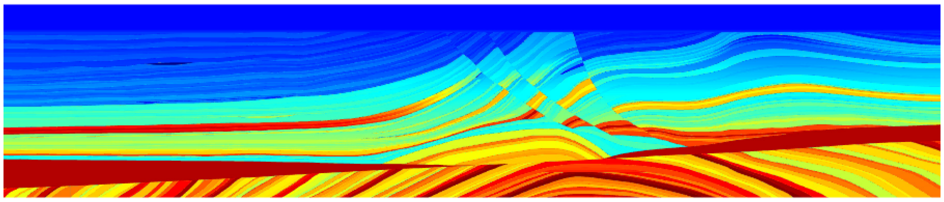

(a) The Marmousi model

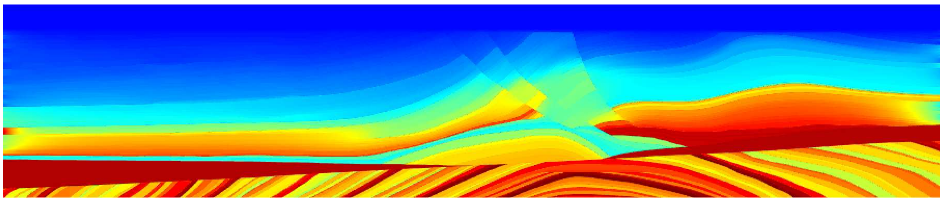

(b) φ_0 with a relative L^2 error of 12.8%

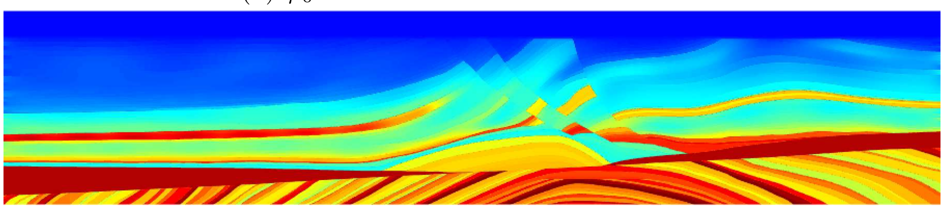

(c) $Q^{\varepsilon}_{100}[u_\delta](u_\delta)$ with a relative L^2 error of 3.8%

Figure 12: The original Marmousi model with its background φ_0 and AS decomposition with 100 eigenfunctions.

As a result we have that for every $x \in \mathcal{B}$, there exists $y > f(x)$ such that $(x, y) \in G(\delta)$, and, in particular, we obtain estimates of $y - f(x)$.

Proposition B.3. *For each $x \in \mathcal{B}$, there exists $t \in [\delta, \Lambda_0\delta]$, with $\Lambda_0 = \sqrt{1 + \Lambda^2}$, such that*

$$(x, f(x) + t) \in G(\delta).$$

Proof. Let $\rho(t) = \operatorname{dist}((x, f(x) + t), \widehat{F})$, $p = (x, f(x))$, and $h_0 = \Lambda_0\delta$. Since

$$\operatorname{dist}(p, (x, f(x) + \delta)) = \delta,$$

we have $\rho(\delta) \leq \delta$. In addition, by Proposition B.2, $\rho(h) > \delta$, for $h > h_0$. Since ρ is continuous, there exists $t \in [\delta, h)$ such that

$$\operatorname{dist}((x, f(x) + t), \widehat{F}) = \rho(t) = \delta \tag{B.7}$$

Because the above is true of every $h > h_0$, we have the conclusion. □

The following proposition puts restrictions on f in a neighborhood of a point $x \in \mathcal{B}$, provided $p = (x, y) \in G(\delta)$. The idea of the proof is illustrated in the right frame of Figure 13.

Proposition B.4. *Let $p = (x, y) \in G(\delta)$, and $\hat{x} \in \hat{\mathcal{B}}$.*

1. If $|\hat{x} - x| \leq \delta$, then

$$f(\hat{x}) \leq y - \sqrt{\delta^2 - |x - \hat{x}|^2}\,. \tag{B.8}$$

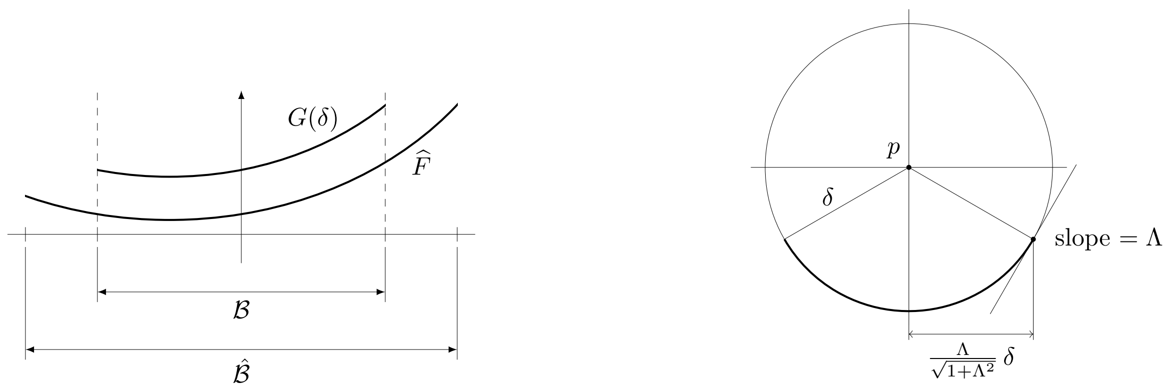

Figure 13: Left: the graph $\widehat{F}$ of f in $\hat{\mathcal{B}}$ and $G(\delta)$; right: illustration of the setup of Proposition B.4 in the plane.

2. If $\operatorname{dist}(p,(\hat{x},f(\hat{x})))=\delta$*, then*

$$|x-\hat{x}| \le \frac{\Lambda\delta}{\sqrt{1+\Lambda^2}} = \frac{\Lambda}{\Lambda_0}\,\delta. \tag{B.9}$$

Proof. 1. Assertion 1 is true because f is continuous, $f(x)<y$, and $\operatorname{dist}(p,\widehat{F})=\delta$.

2. Since $\operatorname{dist}(p,(\hat{x},f(\hat{x})))=\delta$, we have $|x-\hat{x}|\le\delta$ and thus assertion 1 yields

$$f(\hat{x}) = y - \sqrt{\delta^2-|x-\hat{x}|^2}\,. \tag{B.10}$$

By considering the plane containing $p=(x,y)$, $(x,f(x))$ and $(\hat{x},f(\hat{x}))$ (note that these points are indeed distinct), we reduce the problem to the 2-dimensional case ($d=2$). For this case we show assertion 2 by contradiction. Suppose

$$\frac{\Lambda\delta}{\sqrt{1+\Lambda^2}} < |x-\hat{x}| \le \delta. \tag{B.11}$$

It is easy to verify that at $\hat{x}$ the slope of the lower half of the circle centered at $p=(x,y)$ is greater (in absolute value) than Λ (see right frame of Figure 13). Since $\operatorname{dist}(p,\widehat{F})=\delta$ (i.e., the intersection of $\widehat{F}$ with the open ball centered at p is empty), this yields a contradiction to f being Λ-Lipschitz continuous and thus we have the conclusion. □

As a result of Proposition B.4 we have that if $p=(x,y)\in G(\delta)$, then the graph $\widehat{F}$ of f in $\hat{\mathcal{B}}$ lies beneath surface

$$\widetilde{\mathcal{C}} = \big\{r\in\mathcal{B}\times\mathbb{R}:\ \operatorname{dist}\big(r,\mathcal{C}_p^+\big)=\delta\big\} \tag{B.12}$$

illustrated in the right frame of Figure 14, where $\mathcal{C}_p^+$ denotes the upper half of the cone $\mathcal{C}_p$. We use this observation to get the following.

Lemma B.5. *If* $p\in G(\delta)$*, then* $\mathcal{C}_p\cap G(\delta)=\emptyset$*.*

Proof. We show separately the two propositions $\mathcal{C}_p^\pm\cap G(\delta)=\emptyset$, for the upper and lower parts $\mathcal{C}_p^\pm$ of the cone $\mathcal{C}_p$.

1. Consider the lower part $\mathcal{C}_p^-$ of the cone $\mathcal{C}_p$. Since $p=(x,y)\in G(\delta)$, there exists $\hat{p}=(\hat{x},f(\hat{x}))\in\widehat{F}$ such that $\operatorname{dist}(p,\hat{p})=\delta$ and $y>f(\hat{x})$ (by Proposition B.4). Since f is

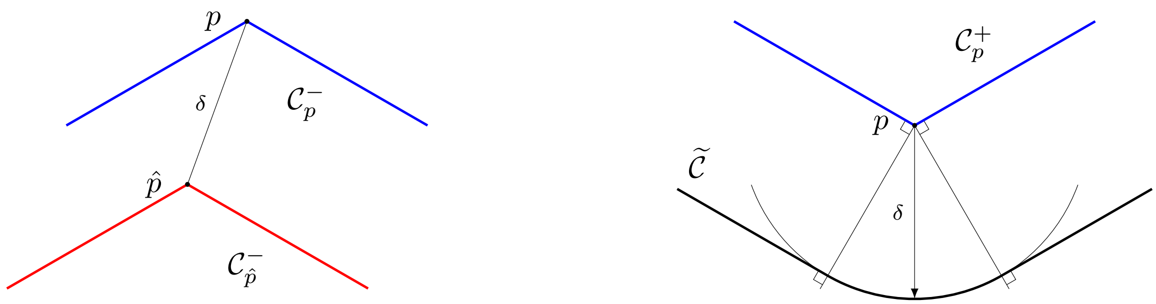

Figure 14: Illustrations for the proof of Lemma B.5; here $\mathcal{C}_p^+$ and $\mathcal{C}_p^-$ denote the upper and lower halves of the cone $\mathcal{C}_p$, respectively

Λ-Lipschitz and $\widehat{F}$ is the graph of f in $\hat{\mathcal{B}}$, we have $\mathcal{C}_{\hat{p}}^- \cap \widehat{F} = \emptyset$, and in particular $\mathcal{C}_{\hat{p}}^-$ lies below $\widehat{F}$. However, the lower part $\mathcal{C}_p^-$ of $\mathcal{C}_p$ is given by $\mathcal{C}_p^- = p - \hat{p} + \mathcal{C}_{\hat{p}}^-$. Since the length of $p - \hat{p}$ is δ, we have that every point r in the interior of $\mathcal{C}_p^-$ is at a distance of δ from a point in the interior of $\mathcal{C}_{\hat{p}}^-$, which yields $\operatorname{dist}(r, \widehat{F}) < \delta$ and thus $r \notin G(\delta)$. Since $r \in \mathcal{C}_p^-$ is arbitrary, we get $\mathcal{C}_p^- \cap G(\delta) = \emptyset$.

2. Now consider the upper part $\mathcal{C}_p^+$ of the cone $\mathcal{C}_p$, and let $r \in \mathcal{C}_p^+$. If $d > 2$, we may reduce the problem to the 2-dimensional case by considering the plane containing r and the vertical line going through p. In the 2-dimensional case, illustrated in the right frame of Figure 14, it is clear that $\operatorname{dist}(r, \widehat{F}) > \delta$, since $\widehat{F}$ lies beneath $\widetilde{\mathcal{C}}$ given by (B.12). □

Theorem B.6. *For $\delta > 0$, the set $G(\delta)$ is the graph of a Λ-Lipschitz function $g : \mathcal{B} \to \mathbb{R}$.*

Proof. By Proposition B.3 and Lemma B.5, for each $x \in \mathcal{B}$, there exists a unique y such that $p = (x, y) \in G(\delta)$. This defines a function $g : \mathcal{B} \to \mathbb{R}$ such that $G(\delta)$ is its graph. Moreover, by Lemma B.5, for each $p \in G(\delta)$, $G(\delta) \cap \mathcal{C}_p = \emptyset$, which yields that g is Λ-Lipschitz. □

B.2 Distance functions for Lipschitz domains

For $r > 0$, let $B(r)$ denote the open ball in $\mathbb{R}^{d-1}$ of radius r centered at the origin.

Proof of Theorem B.1. Since A is Λ-Lipschitz and ∂A is bounded, there is a finite set of pairs (V_n, f_n), with $n = 1, \dots, N$, of bounded open right cylinders V_n and functions f_n of $d-1$ variables satisfying the following:

1. $\{V_n\}_n$ is a finite open cover of ∂A,
2. the bases of V_n are at a positive distance from ∂A,
3. f_n is Λ-Lipschitz, and $f_n(0) = 0$,
4. for each n, there exists a Cartesian coordinate system (ξ, η), with $\xi \in \mathbb{R}^{d-1}$ and $\eta \in \mathbb{R}$, for which
$$V_n = B(r_n) \times (-b_n, b_n), \tag{B.13}$$
for some $r_n, b_n > 0$, and
$$A \cap \hat{V}_n = \{(\xi, \eta) : \ \xi \in B(2r_n),\ f_n(\xi) < \eta < b_n\}, \qquad \hat{V}_n = B(2r_n) \times (-b_n, b_n). \tag{B.14}$$

Choose $\delta > 0$ such that

$$\partial A_\delta \subset \bigcup_{n=1}^{N} V_n \tag{B.15}$$

and for all n, with respect to the n-th coordinate system (ξ, η), the part of the boundary of A_δ lying in V_n coincides with the set $G_n(\delta) = G(\delta)$ given by (B.2) with $f = f_n$, $\mathcal{B} = B(r_n)$, $\hat{\mathcal{B}} = B(2r_n)$. By Theorem B.6, $G_n(\delta)$ is the graph of a Λ-Lipschitz function $g_n : B(r_n) \to \mathbb{R}$. Thus, the boundary ∂A_δ of A_δ is covered by a finite collection of open sets V_n, such that for each n there exists a coordinate system (ξ, η) in which $\partial A_\delta \cap V_n$ coincides with the graph of the Λ-Lipschitz function g_n and $A_\delta \cap V_n$ lies above g_n, which yields the conclusion. □

C Estimates in thin sets

We show the following theorem.

Theorem C.1. *If $A \subset \Omega$ is a Λ-Lipschitz domain, then there exists a constant $C > 0$, such that for every sufficiently small $\delta > 0$ and every $v \in H^1(\Omega)$,*

$$\|v\|^2_{L^2(U_\delta)} \le C \left(\delta^2 \|\nabla v\|^2_{L^2(U_\delta)} + \delta \|v\|^2_{H^1(A_\delta)} \right), \tag{C.1}$$

where

$$U_\delta = \{x \in A : \ \mathrm{dist}(x, \partial A) < \delta\}, \qquad A_\delta = A \setminus \overline{U_\delta}. \tag{C.2}$$

We begin by citing some results of [18] regarding the flattening of Lipschitz graphs. Let V be a bounded domain such that $V \subset \mathcal{B} \times \mathbb{R}$, with $\mathcal{B} \subset \mathbb{R}^{d-1}$ an open ball, and let $f : \mathcal{B} \to \mathbb{R}$ Λ-Lipschitz. We define $Y : V \longrightarrow Y(V)$ by

$$Y(x) = (\hat{x}, x_d - f(\hat{x})) \qquad x = (\hat{x}, x_d) \in \mathcal{B} \times \mathbb{R}. \tag{C.3}$$

Note that the graph of f is mapped by Y to the flat surface $\mathcal{B} \times \{0\}$. It is easy to verify that

$$\left| \det \frac{\partial Y}{\partial x} \right| = 1, \tag{C.4}$$

and that Y is invertible and

$$Y^{-1}(\hat{y}, y_d) = (\hat{y}, y_d + f(\hat{y})). \tag{C.5}$$

We define

$$T : H^1(V) \longrightarrow H^1(Y(V)) \qquad Tu(y) = u\big(Y^{-1}(y)\big). \tag{C.6}$$

The operator T is well defined [18], i.e., for every $u \in H^1(V)$, $Tu \in H^1(Y(V))$. For any summable $g : V \to \mathbb{R}$, by the area formula we have

$$\int_V g(x) dx = \int_{Y(V)} g(Y^{-1}(y)) dy. \tag{C.7}$$

Therefore,

$$\|Tu\|_{L^2(Y(V))} = \|u\|_{L^2(V)}. \tag{C.8}$$

We also have [18]
$$\|\nabla(Tu)\|_{L^2(Y(V))} \le C\|\nabla u\|_{L^2(V)}, \tag{C.9}$$
where C is independent of u and therefore T is continuous from $H^1(V)$ to $H^1(Y(V))$. If

$$\Gamma = \{(\hat{x}, f(\hat{x})) :\ \hat{x} \in \mathcal{B}\} \subset \partial V$$

then there exists $C > 0$ such that for every $u \in H^1(V)$

$$\|Tu\|_{L^2(Y(\Gamma))} \le \|u\|_{L^2(\Gamma)} \le C\|Tu\|_{L^2(Y(\Gamma))}. \tag{C.10}$$

Next we derive PoincarÃľ-type inequalities for functions in cylinders bounded by Lipschitz graphs. Specifically, we are interested in the behavior of the constants of the inequalities with respect to the height of the cylinder.

Lemma C.2. *Let $f : \mathcal{B} \to \mathbb{R}$ be Λ-Lipschitz and for $h > 0$ let*

$$\mathcal{C}_h = \{(\hat{x}, x_d) :\ \hat{x} \in \mathcal{B},\ |x_d - f(\hat{x})| < h\}, \qquad \Gamma_h = \{(\hat{x}, f(\hat{x}) + h) :\ \hat{x} \in \mathcal{B}\}.$$

There exists a constant $C > 0$, such that for every $h > 0$, and $v \in H^1(\mathcal{C}_h)$,

$$C\|v\|^2_{L^2(\mathcal{C}_h)} \le h^2\|\nabla v\|^2_{L^2(\mathcal{C}_h)} + h\,\|v\|^2_{L^2(\Gamma_h)}. \tag{C.11}$$

Proof. Fix $h > 0$ and let $\mathcal{C} = \mathcal{C}_h$ and $\Gamma = \Gamma_h$. The estimate for $f \equiv 0$ follows easily from standard estimates for the smallest eigenvalue λ of the problem

$$-\Delta u = \lambda u \qquad \text{in} \quad \mathcal{C} \tag{C.12}$$
$$\partial_n u = -h^{-1}u \qquad \text{on} \quad \Gamma \tag{C.13}$$
$$\partial_n u = 0 \qquad \text{on} \quad \partial\mathcal{C} \setminus \Gamma. \tag{C.14}$$

Suppose f is Λ-Lipschitz. Then $Y(\mathcal{C}) = \mathcal{B} \times (-h, h)$, and $Y(\Gamma) = \mathcal{B} \times \{h\}$. Since $Y(\mathcal{C})$ is a standard right cylinder, we get

$$\|Tv\|^2_{L^2(Y(\mathcal{C}))} \le C\left(h^2\|\nabla(Tv)\|^2_{L^2(Y(\mathcal{C}))} + h\|Tv\|^2_{L^2(Y(\Gamma))}\right). \tag{C.15}$$

Due to (C.8), (C.9) and (C.10) we get the conclusion. □

We now can prove Theorem C.1

Proof of Theorem C.1. Let $v \in H^1(\Omega)$. Fix $x \in \partial A$. Since A is bounded and Λ-Lipschitz, there exists a cylinder $\mathcal{C}$ and a Λ-Lipschitz function f of $d-1$ variables such that $f(0) = 0$, the bases of $\mathcal{C}$ are at a positive distance from ∂A, and there exists a Cartesian coordinate system (ξ, η), with $\xi \in \mathbb{R}^{d-1}$ and $\eta \in \mathbb{R}$, in which

$$\mathcal{C} = B(r) \times (-b, b), \tag{C.16}$$

for $r, b > 0$, $B(r) \in \mathbb{R}^{d-1}$ the ball of radius r centered at zero and

$$A \cap \mathcal{C} = \{(\xi, \eta) :\ \xi \in B(r),\ f(\xi) < \eta < b\}. \tag{C.17}$$

For $\kappa > 0$, let V_κ denote

$$V_\kappa = \{(\xi,\eta) : \ \xi \in B(r), \ 0 < \eta - f(\xi) < \kappa\}. \tag{C.18}$$

Choose $\delta_0 > 0$ such that $\kappa_0 = 2\delta_0\sqrt{1+\Lambda^2} < b$, and set $\kappa = \Lambda\delta$, for $\delta < \delta_0$. Then, by Proposition B.2 we have

$$U_\delta \cap V_\kappa = U_\delta \cap \mathcal{C} \tag{C.19}$$

and

$$\widetilde{V} = \{(\xi,\eta) : \ \xi \in B(r), \ \kappa < \eta - f(\xi) < \kappa_0\} \subset A_\delta. \tag{C.20}$$

Lemma C.2 yields

$$C\|v\|^2_{L^2(V_\kappa)} \leq \kappa^2 \|\nabla v\|^2_{L^2(V_\kappa)} + \kappa \|v\|^2_{L^2(\Gamma)} \tag{C.21}$$

where

$$\Gamma = \{(\xi, f(\xi) + \kappa) : \ \xi \in B(r)\}.$$

Since κ is bounded at a positive distance below κ_0, we have

$$\|v\|^2_{L^2(\Gamma)} \leq C\|v\|^2_{H^1(\widetilde{V})}. \tag{C.22}$$

Combining the above we obtain

$$C_1\|v\|^2_{L^2(V_\kappa)} \leq \kappa^2 \|\nabla v\|^2_{L^2(V_\kappa)} + \kappa \|v\|^2_{H^1(\widetilde{V})} \tag{C.23}$$

Since $V_\kappa \subset \mathcal{C} \cap A$, we have

$$\|\nabla v\|^2_{L^2(V_\kappa)} \leq \|\nabla v\|^2_{L^2(\mathcal{C}\cap A)} = \|\nabla v\|^2_{L^2(\mathcal{C}\cap U_\delta)} + \|\nabla v\|^2_{L^2(\mathcal{C}\cap A_\delta)} \tag{C.24}$$

Substituting this into (C.23) and using $\widetilde{V} \subset \mathcal{C} \cap A_\delta$ yields

$$C\|v\|^2_{L^2(V_\kappa)} \leq \delta^2 \|\nabla v\|^2_{L^2(U_\delta)} + \delta(1+\delta)\|v\|^2_{H^1(\mathcal{C}\cap A_\delta)}. \tag{C.25}$$

Since ∂A is compact, we can cover it by a finite number of neighborhoods $\mathcal{C}$, independent of δ and thus obtain

$$C\|v\|^2_{L^2(U_\delta)} \leq \delta^2 \|\nabla v\|^2_{L^2(U_\delta)} + \delta(1+\delta)\|v\|^2_{H^1(A_\delta)} \tag{C.26}$$

which completes the proof □

References

[1] Maya de Buhan and Axel Osses. Logarithmic stability in determination of a 3D viscoelastic coefficient and a numerical example. *Inverse Problems*, 26(9):095006, 2010.

[2] Maya de Buhan and Marie Kray. A new approach to solve the inverse scattering problem for waves: combining the TRAC and the adaptive inversion methods. *Inverse Problems*, 29(8):085009, 2013.

[3] Marcus Grote, Marie Graff-Kray, and Uri Nahum. Adaptive eigenspace method for inverse scattering problems in the frequency domain. *Inverse Problems*, 33:025006, 02 2017.

[4] Marcus J. Grote and Uri Nahum. Adaptive eigenspace for multi-parameter inverse scattering problems. *Computers and Mathematics with Applications*, 2019.

[5] Daniel H Baffet, Marcus J Grote, and Jet Hoe Tang. Adaptive spectral decompositions for inverse medium problems. *Inverse Problems*, 37(2):025006, jan 2021.

[6] Martin Burger, Guy Gilboa, and Michael Moeller. Nonlinear spectral analysis via one-homogeneous functionals: Overview and future prospects. *Journal of Mathematical Imaging and Vision*, 56(2):300–319, 2016.

[7] Daniel Cremers, Guy Gilboa, Lina Eckardt, Martin Burger, and Michael Möller. Spectral decompositions using one-homogeneous functionals. *CoRR*, abs/1601.02912, 2016.

[8] G. Bellettini, V. Caselles, and M. Novaga. The total variation flow in $\mathbb{R}^N$. *Journal of Differential Equations*, 184(2):475 – 525, 2002.

[9] Maja de Buhan and Marion Darbas. Numerical resolution of an electromagnetic inverse medium problem at fixed frequency. *Computers and Mathematics with Applications*, 74:3111 – 3128, 2017.

[10] M. Graff, M. J. Grote, F. Nataf, and F. Assous. How to solve inverse scattering problems without knowing the source term: a three-step strategy. *Inverse Problems*, 35:1041001, 2019.

[11] Florian Faucher, Otmar Scherzer, and Hélène Barucq. Eigenvector models for solving the seismic inverse problem for the Helmholtz equation. *Geophysical Journal International*, 221(1):394–414, 01 2020.

[12] Alfio Quateroni. *Numerical Models for Differential Problems*. Springer, 4 edition, 2008.

[13] Lawrence C. Evans and Ronald F. Gariepy. *Measure Theory and Fine Properties of Functions*. CRC Press, 1992.

[14] A. Boulkhemair and A. Chakib. On the uniform poincaré inequality. *Communications in Partial Differential Equations*, 32(9):1439–1447, 2007.

[15] Dirk Pieter Laurie. Algorithm 584: Cubtri: Automatic cubature over a triangle. *ACM Transactions on Mathematical Software (TOMS)*, 8(2):210–218, 1982.

[16] Gary S Martin, Robert Wiley, and Kurt J Marfurt. Marmousi2: An elastic upgrade for marmousi. *The leading edge*, 25(2):156–166, 2006.

[17] Agl elastic marmousi. https://wiki.seg.org/wiki/AGL_Elastic_Marmousi.

[18] Zhonghai Ding. A proof of the trace theorem of sobolev spaces on lipschitz domains. *Proceedings of the American Mathematical Society*, 124(2):591–600, 1996.